PHYSICAL REVIEW D **96,** 063509 (2017)

Emergent scale symmetry: Connecting inflation and dark energy

Javier Rubio[*] and Christof Wetterich[†]

Institut für Theoretische Physik, Ruprecht-Karls-Universität Heidelberg, Philosophenweg 16, 69120 Heidelberg, Germany

(Received 7 May 2017; published 13 September 2017)

Quantum gravity computations suggest the existence of an ultraviolet and an infrared fixed point where quantum scale invariance emerges as an exact symmetry. We discuss a particular *variable gravity* model for the crossover between these fixed points which can naturally account for inflation and dark energy, using a single scalar field. In the Einstein-frame formulation, the potential can be expressed in terms of Lambert functions, interpolating between a power-law inflationary potential and a mixed-quintessence potential. For two natural heating scenarios, the transition between inflation and radiation domination proceeds through a "graceful reheating" stage. The radiation temperature significantly exceeds the temperature of big bang nucleosynthesis. For this type of model, the observable consequences of the heating process can be summarized in a single parameter, the heating efficiency. Our quantitative analysis of compatibility with cosmological observations reveals the existence of realistic models able to describe the whole history of the Universe using only a single metric and scalar field and involving just a small number of order 1 parameters.

DOI: 10.1103/PhysRevD.96.063509

I. INTRODUCTION

A dynamical scalar field with a sufficiently flat potential and at most tiny couplings to ordinary matter is often advocated as a promising alternative to the cosmological constant [1,2]. This idea, usually named quintessence, can partly be viewed as a late-time implementation of the successful inflationary paradigm. Since inflation and dark energy share many essential properties, it is natural to seek for a unification of these two mechanisms into a common framework [3–5]. In this paper, we postulate that inflation and dark energy are intimately related to an underlying symmetry: scale invariance.

When dealing with scale invariance, one can take two different perspectives: (i) assume that scale invariance remains an exact symmetry even when quantum corrections are taken into account [6] or (ii) assume that scale invariance is broken by quantum effects but will be approximately realized *close to fixed points* [1]. Cosmological models based on the first line of reasoning and their associated phenomenology can be found in Refs. [7–17]. Cosmological models of the second type resulting in a dilatation anomaly that vanishes asymptotically in the infinite future led to the first proposal of dynamical dark energy or quintessence [1,18].

In this work, we will adopt the second point of view. In particular, we will assume that scale invariance is generically broken by the conformal anomaly, but it reemerges as an exact quantum symmetry in the early- and late-time evolution of the Universe. The resurgence of the symmetry can be related to the presence of UV and IR fixed points in the renormalization group flow. In the vicinity of these points, any information about the mass scales in the theory is lost [19]. This idea can be easily implemented in a variable gravity scenario [19–21].

In this paper, we present the complete cosmological history for a particular *crossover variable gravity* model with a singlet scalar field. In the *scaling frame*, the field is coupled nonminimally to gravity and to the Standard Model, supplemented by some unspecified dark matter candidate and potentially by heavy particles as in grand unification. The model contains no tiny or huge dimensionless quantities put in by hand. The four parameters appearing in the effective action are all of order 1. The first three describe the approach to the UV and IR fixed points *in the scalar sector* and the position on the crossover trajectory. The last parameter describes the present growth rate of neutrino masses, which is associated to the coupling between the scalar field and neutrinos. For early cosmology, the net effect of the interactions between the scalar field and the Standard Model particles (and possible sectors beyond that) can be summarized in a *heating efficiency* Θ. These few parameters are sufficient for a quantitative account of the history of the Universe from inflation to the present accelerated expansion era. Our simple model seems so far compatible with cosmological observations. Neither tiny or fine-tuned parameters are introduced to explain the small value of the present dark energy density, which is rather a consequence of the long age of the Universe in Planck units.

The comparison of our model with cosmological observations is performed in the Einstein frame with a canonical kinetic term for the scalar field. This allows us to find

[*]j.rubio@thphys.uni-heidelberg.de
[†]c.wetterich@thphys.uni-heidelberg.de

explicit analytic solutions and facilitates the comparison with other quintessential inflation models in the literature; see for instance Refs. [3–5] for well-known examples and Refs. [22–25] for recent discussions. We follow here the general approach in which the inflationary epoch is followed by a transition to a scaling or tracker solution of which the long duration is responsible for the tiny value of the present dark energy density. The end of this scaling era is triggered by neutrinos with growing masses that become nonrelativistic in the recent cosmological history. This general scenario, originally proposed in Refs. [21,26], has been recently followed by several groups [22–25]. The explicit Einstein-frame formulation presented in this paper allows us to replace arguments for approximate solutions by exact analytical results, which substantially extends the range of validity of the scenario in parameter space.

Beyond the explicit and convenient solutions in the Einstein frame, our investigation contains several new results. We propose for the *heating* or entropy production preceding the radiation dominated epoch a general mechanism that is neither gravitational particle production nor instant preheating. Only the latter two mechanisms have been previously discussed within models of quintessential inflation. The mechanism presented in this paper is based on the general framework for particle production in the presence of time-varying fields but adapted to the situation in which the potential does not have a minimum. The absence of a minimum is required for the transition from inflation to a tracker solution and typical for a variable gravity framework containing a single crossover at early times. For this scenario, all features relevant for observations can be summarized into a single parameter: the heating efficiency Θ. The duration of the kination epoch between the end of inflation and the onset of the radiation dominated epoch can be rather short, leading to a high heating temperature. We find that the (almost massless) cosmon excitations generated during the heating stage do not significantly contribute to the effective number of neutrino species at big bang nucleosynthesis.

This paper is organized as follows. In Sec. II, we present the effective action of the model in a scaling frame where the Planck mass is given by a scalar field. We describe the properties of the UV and IR fixed points responsible for the early- and late-time acceleration of the Universe. In Sec. III, we reformulate the variable gravity scenario into the more common, although completely equivalent, Einstein frame. This formulation is used in the following sections to study the cosmological implications of the model. Section IV contains the details of inflation. We show that the UV fixed point gives rise to a power-law Einstein-frame potential and derive the associated inflationary observables. The spectral tilt and the tensor-to-scalar ratio are shown to be related and to depend only on the UV fixed-point anomalous dimension. The initial stages of the postinflationary dynamics are discussed in Sec. V. The crossover to the IR fixed point translates into the appearance of a field region where the Einstein-frame potential becomes steep. This triggers the onset of a kinetic domination regime. The kinetic regime must be limited in time for the model to be cosmologically viable. In particular, part of the energy density of the inflaton field must be transmitted to the Standard Model particles, which must become the dominant energy component before big bang nucleosynthesis (BBN). In Sec. VI, we discuss two natural heating mechanisms and determine the associated radiation temperature ("reheating" temperature). We argue that a total decay of the inflaton field is not possible and is neither necessary nor even preferable. The evolution after heating and the onset of the dark energy dominated era are discussed in Sec. VII. Section IX contains our conclusions. Appendix A summarizes several properties of Lambert functions that are useful for the derivation of the analytic solutions presented in this paper. Appendixes B and C contain details of our heating scenario and of the creation of cosmon excitations during this period.

II. VARIABLE GRAVITY SCENARIO

The variable gravity scenario is usually formulated in a scaling frame in which not only the Planck scale but also the dimensionless couplings and masses of elementary particles are allowed to depend on the expectation value of a scalar field χ. We consider here a simple real scalar which plays simultaneously the role of the inflaton, the cosmon, or the dilaton. The effective Lagrangian density for the graviscalar sector of the theory reads [19–21]

$$\frac{\mathcal{L}}{\sqrt{-\tilde{g}}}=\frac{\chi^2}{2}\tilde{R}-\frac{B(\chi/\mu)-6}{2}(\tilde{\partial}\chi)^2-\mu^2\chi^2, \tag{1}$$

where the tilde denotes quantities in the scaling frame and we have suppressed Lorentz indices. The implicit contractions in this paper should be understood in terms of the metric associated with the frame under consideration.

The cosmon field χ in Eq. (1) defines the effective *variable* Planck mass. We will see that for the cosmological solutions of the field equations derived from the action (1) it increases with time, with $\chi(t\to-\infty)\to 0$ and $\chi(t\to\infty)\to\infty$. The only fixed scale not proportional to the cosmon field is the scale μ, which is associated to the scale or dilatation anomaly. The value of μ has no intrinsic meaning and can be used to set the mass scales. We will take

$$\mu^{-1}=10^{10}\ \text{yr}=1.2\times 10^{60}M_P^{-1}. \tag{2}$$

For this choice, the present value of the variable Planck mass in Eq. (1) amounts to $M_P=\chi(t_0)=2.48\times 10^{18}$ GeV [21]. In other words, the increasing ratio χ/μ has reached today a value 1.2×10^{60}.

We have chosen to normalize the scalar field by its coupling to curvature in the scaling frame, i.e., by the first term in the right-hand side of Eq. (1). With this normalization, the scalar kinetic term has typically a nonstandard normalization, as reflected by the dimensionless function $B(\chi/\mu)$. In order to have a well-defined kinetic term during the whole cosmological evolution, we will require the function B to be a positive function of χ/μ. For $\mu = 0$ and constant B, the associated action is scale invariant, while for $B = \mu = 0$, the action is also conformally invariant, and the cosmon field χ no longer propagates.

For the matter and radiation sectors, we take the Standard Model of particle physics with possible extensions including dark matter. We assume that at large χ the values of all the (renormalizable) dimensionless couplings in the Standard Model become independent of χ, as required by scale symmetry. In practice, this implies that the Fermi scale and the confinement scale of strong interactions are proportional to χ. The masses and binding energies of all elementary particles are then proportional to the dilaton expectation value, while cross sections scale as χ^{-2}. In consequence, our setting is compatible with the equivalence principle tests and the severe bounds on the variation of fundamental constants [27].

A recent quantum gravity computation based on functional renormalization has indeed found for variable gravity a quadratic increase of the scalar potential for large χ [28]. A strong enhancement of the effect of long-distance graviton fluctuations avoids a potential instability of the graviton propagator that would arise for a potential increasing faster than χ^2. More generally, large classes of effective actions containing no more than two derivatives can be brought to the form (1) by appropriate nonlinear field redefinitions [19]. For example, this concerns potentials of the form $V = \alpha\mu^4 + \mu^2\chi^2$.

A given model is specified by a choice of $B(\chi/\mu)$. For successful quintessential inflation, one needs large B during the inflationary epoch and small B after the end of inflation. Large B ensures slow-roll dynamics during inflation, while inflation ends once B gets small. In this paper, we will concentrate on a particular scenario where B satisfies the flow equation

$$\mu\frac{\partial B}{\partial\mu} = \frac{\kappa\sigma B^2}{\sigma + \kappa B}. \tag{3}$$

This equation contains an infrared fixed point $B_* = 0$, approached for $B \to 0$ with a quadratic term

$$\mu\partial_\mu B = \kappa B^2. \tag{4}$$

The ultraviolet fixed point for $B \to \infty$,

$$\mu\partial_\mu B = \sigma B, \tag{5}$$

is characterized by an anomalous dimension σ.

No quantum gravity computation for the flow of B is available so far. Equation (3) should be therefore understood as an educated guess, or an assumption, on the exact quantum gravity dynamics. As suggested by the first investigations in Ref. [29], we assume the renormalization flow of quantum gravity to admit both an UV and an IR fixed point. The enhanced conformal symmetry for $B = \mu = 0$ implies that the β-function for B vanishes for $B = 0$. If the β-function in the IR limit is analytic in B around $B = 0$, i.e., $B = \sigma_{\rm IR}B + \kappa B^2$, the assumption of a vanishing infrared anomalous dimension $\sigma_{\rm IR} = 0$ motivates the limit (4). A simple way of achieving large B in the UV limit is an anomalous dimension of the scalar wave function renormalization, leading to the limit (5). The precise interpolation between the UV and IR fixed points in Eq. (3) is not important for the observable consequences of the model. A reason for the selection of the particular crossover in Eq. (3) is its simplicity. The scalar-gravity sector contains only three order 1 parameters: two constants σ and κ and an integration constant c_t selecting a particular trajectory in the flow. The resulting tensor-to-scalar ratio of primordial perturbations turns out to be comparatively large, $r \simeq 0.05$–0.1 [19] (see also Ref. [22]). Smaller values of r can be obtained by modifying the behavior of B at small χ, for example by assuming a fixed point of the flow at some large but finite B_* [26], instead of the limit (5).

Since the main points of this paper will not be affected by the details of the function B, we will take advantage of the simplicity of Eq. (3) for finding explicit solutions. Indeed, Eq. (3) can be easily integrated to obtain

$$\frac{\sigma}{\kappa B} + \ln\frac{\sigma}{\kappa B} = \ln\left[\frac{\sigma}{\kappa}\left(\frac{\chi}{m}\right)^\sigma\right], \tag{6}$$

or equivalently [cf. Eq. (A2)]

$$\frac{\sigma}{\kappa B(\chi)} = \mathcal{W}\left[\frac{\sigma}{\kappa}\left(\frac{\chi}{m}\right)^\sigma\right], \tag{7}$$

with $\mathcal{W}$ the Lambert function [30] and

$$m \equiv \mu\exp(c_t), \tag{8}$$

a *crossover* scale related to the integration constant c_t via dimensional transmutation.

III. EINSTEIN-FRAME FORMULATION

Most of the literature on inflation and on dynamical dark energy employs a canonically normalized scalar field in the Einstein frame. In order to permit an easy access and comparison of models for a wider community, the investigations and results of the present paper will be performed

in this setting. The transformation of our variable gravity scenario to the Einstein frame will be done in two steps. The first realizes the Einstein frame with a fixed Planck mass M_P and a noncanonically normalized scalar field. The second step proceeds to a canonical normalization of the scalar kinetic term.

Performing a conformal transformation $g_{\mu\nu} = (\mu^2/M_P^2)V^{-1}(\chi(\varphi))\tilde{g}_{\mu\nu}$, with dimensionless scalar potential

$$V(\chi(\varphi)) = \left(\frac{\mu}{\chi}\right)^2 = e^{-\alpha\varphi/M_P}, \tag{9}$$

and reduced Planck mass $M_P = 2.435 \times 10^{18}$ GeV, we obtain

$$\frac{\mathcal{L}}{\sqrt{-g}} = \frac{M_P^2}{2}R - \frac{1}{2}k^2(\varphi)(\partial\varphi)^2 - M_P^4 V(\varphi), \tag{10}$$

with

$$k^2(\varphi) = \frac{\alpha^2}{4}B(\varphi), \tag{11}$$

$$B(\varphi) = \frac{\sigma}{\kappa}\mathcal{W}^{-1}\left[\frac{\sigma}{\kappa}\left(\frac{m}{\mu}\right)^{-\sigma}\exp\left(\frac{\alpha\sigma\varphi}{2M_P}\right)\right]. \tag{12}$$

The constant α in Eq. (11) can be chosen to get the standard normalization ($k^2 = 1$) in the present cosmological epoch [26],

$$\alpha^2 = \frac{4}{B(\chi = M_P)} \approx 4\kappa\ln(M_P/m). \tag{13}$$

One could also take $\alpha = 1$. As we will see below, the constant α will completely disappear after canonically normalizing the scalar kinetic term.

Due to the positive definite choice of B in Eq. (1), the Einstein-frame Lagrangian (10) is ghost free. In this basis, the cosmon potential $V(\varphi)$ decays exponentially to zero [1,18], and the dynamical information is encoded in the *kinetial* $k^2(\varphi)$ [20,26]; see also Ref. [31]. The kinetic term can be made canonical by performing an additional field redefinition,

$$\frac{d\phi}{d\varphi} = k(\varphi). \tag{14}$$

The relation between ϕ and χ is given by (see also Fig. 1)

$$V = \left(\frac{\mu}{\chi}\right)^2 = V_0\left[\frac{\exp(-Y)}{Y}\right]^{2/\sigma}, \tag{15}$$

with

$$Y = \frac{\sigma}{\kappa B(\chi)} = 1 + \frac{1}{2}\left[\frac{\phi^2}{\phi_t^2} + \frac{\phi}{\phi_t}\sqrt{4 + \frac{\phi^2}{\phi_t^2}}\right]. \tag{16}$$

Here,

$$V_0 = \left(\frac{\mu}{m}\right)^2\left(\frac{\sigma}{\kappa}\right)^{2/\sigma}, \tag{17}$$

and

$$\phi_t \equiv \frac{2M_P}{\sqrt{\kappa\sigma}} \tag{18}$$

denotes a *transition* field value lying between the UV and IR fixed points. Indeed, Eq. (15) implies

$$Ye^Y = \frac{\sigma}{\kappa}\left(\frac{\chi}{m}\right)^\sigma. \tag{19}$$

This equation allows us to identify Y with the Lambert function in Eq. (7) and establishes the first equality in Eq. (16). For the relation between Y and ϕ, we take into account that

$$\frac{d\phi}{dY} = \frac{d\phi}{d\varphi}\frac{d\varphi}{d\chi}\frac{d\chi}{dY} = \frac{M_P}{\chi}\sqrt{B}\frac{d\chi}{dY} \tag{20}$$

$$= \frac{\phi_t}{2}(Y^{-1/2} + Y^{-3/2}). \tag{21}$$

Integrating this expression, we get the identity

$$\frac{\phi}{\phi_t} = Y^{1/2} - Y^{-1/2}, \tag{22}$$

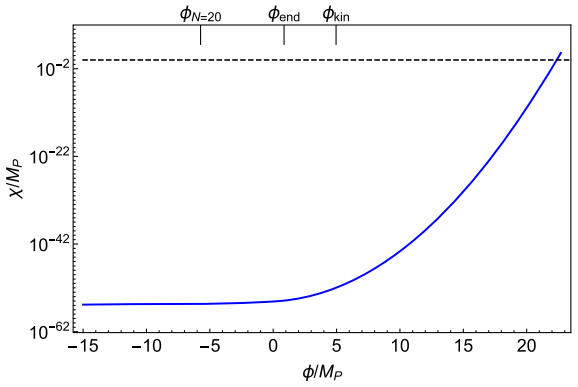

FIG. 1. The relation between χ and ϕ given by Eq. (15). For this figure, we took $\sigma = 4$, $\kappa = 1$, and $m = 10^5\mu$ with μ given by Eq. (2). The black-dashed line corresponds to $\chi = M_P$. For reference, we indicate the values of the field ϕ (in M_P units) at $N = 20$ e-folds before the end of inflation ($\phi_{N=20}$), at the inflationary exit ($\phi_{\rm end}$), and at the onset of the kinetic domination regime ($\phi_{\rm kin}$).

which can be easily inverted to obtain the second equality in Eq. (16). The relation between φ and ϕ follows from $\varphi(\chi)$ in Eq. (9) and $\chi(Y(\phi))$ as given by Eqs. (15) and (16).

In the canonical basis, the action takes the standard form

$$\frac{\mathcal{L}}{\sqrt{-g}} = \frac{M_P^2}{2}R - \frac{1}{2}(\partial\phi)^2 - M_P^4 V(\phi). \tag{23}$$

All dynamical information is now encoded in the effective potential $M_P^4 V(\phi)$, as given by Eqs. (15) and (16). The second term in Eq. (16) contains a linear piece in ϕ. The potential $V(\phi)$ in Eq. (15) is therefore nonsymmetric for arbitrary σ. For $\phi \ll -\phi_t$, one gets $Y \approx \phi_t^2/\phi^2$, and Eq. (15) becomes a power-law (chaotic) potential,

$$V(\phi) \simeq V_0 \left(\frac{\phi^2}{\phi_t^2}\right)^{2/\sigma} = A\left(\frac{\phi^2}{M_P^2}\right)^{2/\sigma}, \tag{24}$$

with

$$A \equiv \left(\frac{\mu}{m}\right)^2 \left(\frac{\sigma}{2}\right)^{4/\sigma}. \tag{25}$$

On the other hand, for $\phi \gg \phi_t$, one has $Y \approx \phi^2/\phi_t^2 + 2$, and $V(\phi)$ can be approximated by a mixed-quintessence potential,

$$V(\phi) \simeq V_0 \left[\frac{\exp(-\frac{\phi^2}{\phi_t^2} - 2)}{\frac{\phi^2}{\phi_t^2} + 2}\right]^{2/\sigma}. \tag{26}$$

The comparison between the exact cosmon potential (15) and the approximated expressions (24) and (26) is shown in Fig. 2.

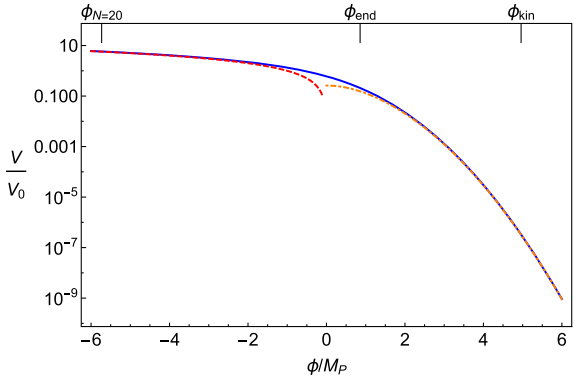

FIG. 2. The cosmon potential for $\sigma = 4$ and $\kappa = 1$. The blue line corresponds to the exact expression (15), while the orange-dotted line and red-dashed lines are associated to the approximated expressions (26) and (24) respectively. For reference, we indicate the values of the cosmon field ϕ (in M_P units) at $N = 20$ e-folds before the end of inflation ($\phi_{N=20}$), at the inflationary exit ($\phi_{\rm end}$), and at the onset of the kinetic domination regime ($\phi_{\rm kin}$).

We recall that ratio μ/m in Eq. (25) is related to the integration constant c_t determining the particular trajectory in the flow [cf. Eq. (8)]. Order 1 values of c_t translate naturally into values of A that are exponentially smaller than one, $A \sim \exp(-2c_t)$. This provides for a natural explanation of the small amplitude of the primordial fluctuations.

IV. INFLATIONARY ERA

We can now proceed to discuss the observable consequences of our model by using the standard methods developed for a canonically normalized scalar field in the Einstein frame. If correctly defined and computed, the observable predictions cannot depend on the particular frame under consideration nor on the precise scalar-field normalization. This is indeed verified by the following independent computations. These computations put our variable gravity framework in direct contact with the known properties of inflationary potentials and dynamical dark energy scenarios existing in the literature.

The approximate power-law form of the potential at $\phi \ll -\phi_t$ allows for inflation with the usual chaotic initial conditions. The Einstein-frame equation of motion for the cosmon field in a flat Friedmann-Lemaître-Robertson-Walker Universe,

$$ds^2 = -dt^2 + a^2(t)d\mathbf{x}^2, \tag{27}$$

is given by

$$\ddot{\phi} + 3H\dot{\phi} + M_P^4 V_{,\phi} = 0, \tag{28}$$

with dots denoting derivatives with respect to the coordinate time t and $H = \dot{a}(t)/a(t)$. The Universe undergoes a phase of accelerated expansion if

$$\epsilon_H \equiv -\frac{\dot{H}}{H^2} < 1. \tag{29}$$

The evolution of the acceleration parameter (29) can be determined by numerically solving Eq. (28) together with the Friedmann equations and standard slow-roll initial conditions. Depending on the value of ϕ_t, the end of inflation for the inflationary potentials (15) and (24) can take place at slightly different field values (the smaller the transition scale ϕ_t, the smaller the difference). This change translates into a small variation in the number of e-folds for the values of κ and σ we are interested in. Having this in mind, we will estimate the inflationary observables using the simple power-law approximation (24). Following the standard procedure, we obtain the following expressions for the spectral tilt and the tensor-to-scalar ratio,

$$1 - n_s = \frac{2+\sigma}{\sigma N + 1}, \qquad r = \frac{16}{\sigma N + 1}, \tag{30}$$

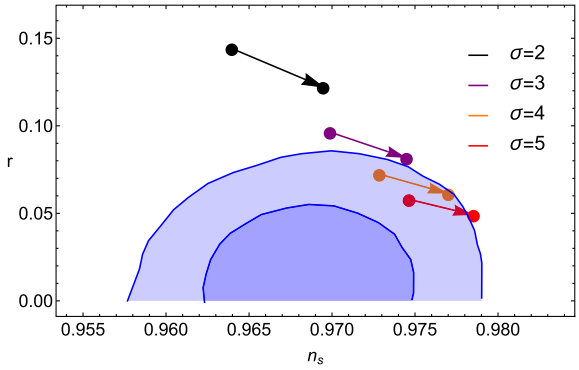

FIG. 3. Comparison between the inflationary predictions (30) and the latest Planck/BICEP2 data at 68% and 95% C.L. [32,33]. The arrows go from the values obtained assuming $N = 55$ e-folds to those for $N = 65$ (cf. Sec. VII B for a more precise estimation of the number of e-folds). For $\sigma \gtrsim 4$, the predicted spectral tilt and tensor-to-scalar ratio lay inside the 2σ contour.

with

$$N = \frac{\sigma}{8M_P^2}[(\phi_{\rm hc})^2 - (\phi_{\rm end})^2], \tag{31}$$

the number of e-folds between the horizon crossing of the relevant fluctuations ($\phi = \phi_{\rm hc}$) and the end of inflation ($\phi_{\rm end}/M_P = 2\sqrt{2}/\sigma$). These Einstein-frame results improve the estimates in Ref. [19] by properly identifying the end of inflation with $\epsilon_H \approx \epsilon_V = 1$.[1] The comparison of (30) with the latest cosmic microwave background (CMB) results is shown in Fig. 3. For an anomalous dimension $\sigma \gtrsim 4$, the inflationary predictions lay within the 2σ Planck/BICEP2 contour [32,33].

The amplitude of scalar perturbations

$$\mathcal{A} = \frac{V(\phi_{\rm hc})}{rM_P^4} = 3.56 \times 10^{-8}, \tag{32}$$

together with Eqs. (24) and (30) evaluated at horizon crossing ($\phi = \phi_{\rm hc}$), determine the ratio

$$\frac{m}{\mu} = 2^{\frac{1}{\sigma}-2}(\sigma N + 1)^{\frac{1}{2}+\frac{1}{\sigma}}\mathcal{A}^{-\frac{1}{2}} \tag{33}$$

and the associated trajectory in the flow. For $\sigma = 4$ and $N = 60$, one obtains $m \simeq 10^5\mu$. Our results agree with Ref. [19].

Once we have determined the Einstein-frame inflationary dynamics, we can always reinterpret our results in terms of the original variable gravity formulation. In particular, it is interesting to compare the value of the cosmon field χ during inflation with the scales μ and m. Combining Eqs. (9) and (32), we get

$$\frac{\chi_{\rm hc}}{\mu} = \frac{1}{\sqrt{\mathcal{A}r}}, \tag{34}$$

meaning that horizon crossing happens when $\chi \gg \mu$. This value is, however, much smaller than m, as can be easily seen by combining Eqs. (24) and (25) and taking into account Eq. (15),

$$\frac{\chi}{m} = \left(\frac{4M_P^2}{\sigma^2\phi^2}\right)^{1/\sigma}. \tag{35}$$

Evaluating the result at horizon crossing, we get

$$\frac{\chi_{\rm hc}}{m} = \left(\frac{4M_P^2}{\sigma^2\phi_{\rm hc}^2}\right)^{1/\sigma} = \left(\frac{r}{32}\right)^{1/\sigma}, \tag{36}$$

with r the tensor-to-scalar ratio in Eq. (30). The scale m is indeed associated to the end of inflation,

$$\frac{\chi_{\rm end}}{m} = \left(\frac{4M_P^2}{\sigma^2\phi_{\rm end}^2}\right)^{1/\sigma} = \frac{1}{2^{1/\sigma}}. \tag{37}$$

A simple overall picture of inflation arises. The inflationary phase corresponds to the vicinity of the UV fixed point for $\chi \lesssim m$. Close to a fixed point, approximate scale symmetry is manifestly realized. This approximate symmetry is the origin of the almost scale invariant primordial fluctuation spectrum. For $\chi \approx m$, one observes the crossover from the vicinity of the UV fixed point to the vicinity of the IR fixed point. Scale invariance is substantially violated in this crossover region. This violation triggers the end of inflation. The scale m is an integration constant of an almost logarithmic flow. Small values of μ/m arise therefore naturally, similarly to the small ratio of the confinement scale in quantum chromodynamics as compared to some "unification scale." This provides for a small fluctuation amplitude,

$$\mathcal{A} = \frac{1}{32}[2(\sigma N + 1)]^{1+\frac{2}{\sigma}}\frac{\mu^2}{m^2}, \tag{38}$$

without the necessity for tuning.

V. KINETIC DOMINATED ERA

After inflation, the inflaton rolls down into the steep potential (26), leading to a substantial decrease of the potential energy density. The evolution of the cosmon field becomes dominated by its kinetic energy, and the heating of the Universe sets in. In this section, we consider the initial epoch in which the energy density into radiation is still small as compared to the energy density of the cosmon.

[1]The estimates in Ref. [19] replace the denominators $\sigma N + 1$ in Eq. (30) by $\sigma N + 3$, due to a small change in the precise definition of the end of inflation. While in the present work, the offset of inflation is defined to occur at $B_{\rm end} = 2$, Ref. [19] takes $B_{\rm end} = 6$.

Such a period is usually referred as *kination* or *deflation* [4]. During this epoch, we can continue to use the cosmon-field equation (28). Neglecting the potential energy density in the first approximation, the equation $\ddot{\phi} + 3H\dot{\phi} \simeq 0$ with $H = 1/(3t)$ admits a solution,

$$\phi(t) = \phi_{\rm kin} + \dot{\phi}_{\rm kin} t_{\rm kin} \log\left(\frac{t}{t_{\rm kin}}\right), \tag{39}$$

with $\phi_{\rm kin}$ and $\dot{\phi}_{\rm kin}$ the value of the field and its derivative at the onset of the kinetic era at $t_{\rm kin}$. During this regime, the cosmon energy density scales as a^{-6}. This behavior is reflected by the cosmon equation of state

$$w_\phi = \frac{p_\phi}{\rho_\phi} = \frac{\frac{1}{2}\dot{\phi}^2 - M_P^4 V}{\frac{1}{2}\dot{\phi}^2 + M_P^4 V} \approx 1. \tag{40}$$

In Fig. 4, we show the numerical solution of the field equations for w_ϕ as a function of the number of e-folds N. The equation of state evolves rapidly toward $w_\phi = 1$ after the end of inflation.

For a realistic cosmology, the kinetic domination regime has to end before big bang nucleosynthesis. For this era to begin, the energy density of the cosmon field must be (dominantly) transmitted to the Standard Model degrees of freedom. In a nonoscillatory model like the one under consideration, a total decay of the inflaton field is not expected since $\dot{\phi} = 0$ is not a solution of the equations of motion in the absence of a minimum. Also, highly effective processes such as parametric resonance cannot take place in a nonoscillatory model.

Although an incomplete inflaton decay would constitute a serious drawback for most inflationary models, it does not in the variable gravity scenario. To understand this, let us assume that a given heating mechanism is able to produce a partial depletion of the cosmon condensate by the creation of relativistic particles. Even if the energy density of this component is initially very small, it will inevitably dominate the energy budget at later times. Indeed, during the kinetic dominated regime, the energy density of the created particles scales as $\rho_{\rm r} \sim a^{-4}$, while that of the cosmon field evolves as a^{-6}. The rapid decrease of the cosmon energy density will inevitably give rise to a late-time domination of the radiation component.

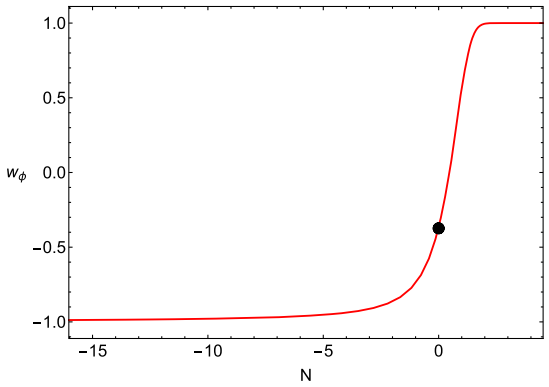

FIG. 4. The cosmon equation of state in the potential (15) with $\sigma = 4$ and $\kappa = 1$ as a function of the number of e-folds N. The end of inflation after 60 e-folds is indicated with a black dot. The limit $w_\phi = 1$ corresponds to a kinetic dominated regime.

The *radiation temperature* $T_{\rm rad}$ at which the energy density of the created particles equals that of the cosmon ($\rho_{\rm r}^{\rm rad} = \rho_\phi^{\rm rad}$) can be defined as

$$T_{\rm rad} \equiv \left(\frac{30\rho_{\rm r}^{\rm rad}}{\pi^2 g_*^{\rm rad}}\right)^{1/4}, \tag{41}$$

with $g_*^{\rm rad}$ the effective number of relativistic degrees of freedom at that temperature. The quantity $T_{\rm rad}$ should be interpreted as the typical energy scale for the onset of radiation domination. It coincides with the heating temperature (usually called the reheating temperature) in the *fast thermalization* limit.

For a simplified scenario, we may assume particle production to take place instantaneously at the onset of the kinetic regime. This motivates the introduction of a heating efficiency, defined in this limit as

$$\Theta \equiv \frac{\rho_{\rm r}^{\rm kin}}{\rho_\phi^{\rm kin}}. \tag{42}$$

We will later extend the definition of Θ to smoother transitions. For the types of heating or entropy production mechanisms considered in this paper, the parameter Θ is sufficient for a quantitative description of the cosmological history.

For instant particle production, the heating efficiency can be easily related to the radiation temperature $T_{\rm rad}$ by taking into account that

$$\Theta = \frac{\rho_{\rm r}^{\rm kin}}{\rho_\phi^{\rm kin}} = \left(\frac{a_{\rm kin}}{a_{\rm rad}}\right)^2. \tag{43}$$

We get

$$T_{\rm rad} = \left(\frac{30\Theta^3\rho_\phi^{\rm kin}}{\pi^2 g_*^{\rm rad}}\right)^{\frac{1}{4}} = \Theta^{\frac{1}{2}}\left(\frac{g_*^{\rm kin}}{g_*^{\rm rad}}\right)^{\frac{1}{4}} T_{\rm kin}, \tag{44}$$

with

$$T_{\rm kin} \equiv \left(\frac{30\rho_{\rm r}^{\rm kin}}{\pi^2 g_*^{\rm kin}}\right)^{1/4}, \tag{45}$$

the temperature of the created particles at the onset of kinetic domination. The longer the kinetic regime, the smaller the radiation temperature $T_{\rm rad}$ is. The heating efficiency (43) must be large enough to avoid conflicts

TABLE I. Approximate values of the Hubble rate at the end of inflation and at the onset of the kinetic dominated era. The numbers displayed were obtained by numerically solving the equations of motion for $\kappa = 1$ and different values of σ. The end of inflation is defined by the condition $\epsilon_H = 1$ with ϵ_H given by Eq. (29). The beginning of the kinetic era is defined by the time at which the effective equation-of-state parameter w_ϕ equals 1, up to one percent accuracy.

σ	ϕ_t/M_p	$H_{\rm end}$ (GeV)	$H_{\rm kin}$ (GeV)
2	$\sqrt{2}$	6.2×10^{12}	5.8×10^{10}
3	$2/\sqrt{3}$	8.9×10^{12}	1.2×10^{11}
4	1	1.1×10^{13}	1.6×10^{11}

with BBN. For the power-law inflationary potential (24), the Hubble rate at the end of inflation/onset of kinetic domination is of order 10^{11}–10^{13} GeV (cf. Table I), with a slight dependence on the precise value of σ. Taking this into account, Eq. (44) becomes

$$\frac{T_{\rm rad}}{10^{14}\ {\rm GeV}} \simeq a\Theta^{3/4}\left(\frac{H_{\rm kin}}{10^{11}}\right)^{1/2}, \tag{46}$$

with $a = 8.65(g_*^{\rm rad})^{-1/4}$.

The inflationary dynamics not only excites cosmon fluctuations but also generates primordial gravitational waves (GW). In the postinflationary era, the amplitude of GW with superhorizon wavelengths remains constant until it reenters the horizon. When that happens, the logarithmic GW spectrum scales as [34]

$$\Omega_{\rm GW}(k) = \frac{1}{\rho_c}\frac{d\rho_{\rm GW}}{d\ln k} \propto k^{2\left(\frac{3w-1}{3w+1}\right)}, \tag{47}$$

with w the effective equation of state. For a radiation dominated expansion, the GW spectrum remains flat. However, for a kinetic dominated regime, the spectrum becomes blue tilted and may eventually dominate the total energy budget.

Nucleosynthesis constraints set an integral bound on the GW density fraction at BBN, namely [35]

$$h^2\int_{k_{\rm BBN}}^{k_{\rm end}} \Omega_{\rm GW}(k) d\ln k \lesssim 10^{-5}, \tag{48}$$

with $h = 0.678$ and $k_{\rm end}$ and $k_{\rm BBN}$ the momenta associated respectively to the horizon scale at the end of inflation and at BBN. The dominant contribution to this integral comes from momenta that left the horizon before the end of inflation and reentered during kinetic domination. For these modes ($k_{\rm rad} < k < k_{\rm kin}$) [36] (see also Refs. [34,37]),

$$\Omega_{\rm GW}(k) = \varepsilon\Omega_\gamma h_{\rm GW}^2\left(\frac{k}{k_{\rm rad}}\right)\ln^2\left(\frac{k}{k_{\rm kin}}\right), \tag{49}$$

with

$$h_{\rm GW}^2 = \frac{1}{8\pi}\left(\frac{H_{\rm kin}}{M_P}\right)^2 \tag{50}$$

the dimensionless amplitude of gravitational waves. The present radiation content in critical units $\rho_c = 1.05 \times 10^{-5} h^2\ {\rm GeV\,cm^{-3}}$ is given by

$$\Omega_\gamma \equiv \frac{\rho_\gamma(t_0)}{\rho_c(t_0)} = 2.6 \times 10^{-5} h^{-2}. \tag{51}$$

The factor

$$\varepsilon = \frac{81}{16\pi^3}\left(\frac{g_{\rm dec}}{g_{\rm th}}\right)^{1/3} \tag{52}$$

takes into account the variation on the number of massless degrees of freedom between thermalization and decoupling [36]. For the Standard Model content ($g_{\rm th} = 106.75$, $g_{\rm dec} = 3.36$), we have $\varepsilon \simeq 0.05$.

Combining Eqs. (48) and (49), and neglecting a subleading logarithmic correction in the $k_{\rm kin} \gg k_{\rm rad}$ limit, we obtain

$$2\varepsilon h^2\Omega_\gamma h_{\rm GW}^2\left(\frac{k_{\rm kin}}{k_{\rm rad}}\right) \lesssim 10^{-5}. \tag{53}$$

The ratio $k_{\rm kin}/k_{\rm rad}$ in this expression can be easily related to Eq. (43) by taking into account that

$$\frac{k_{\rm min}}{k_{\rm rad}} = \frac{a_{\rm kin}H_{\rm kin}}{a_{\rm rad}H_{\rm rad}} = \frac{1}{\sqrt{2}}\left(\frac{\rho_\phi^{\rm kin}}{\rho_{\rm r}^{\rm rad}}\right)^{1/3} = \frac{1}{\sqrt{2\Theta}}. \tag{54}$$

Using these results, the integral bound on the GW density fraction at BBN can be translated into a lower bound on the heating efficiency,

$$\Theta \gtrsim \frac{10^5\varepsilon h^2\Omega_\gamma}{4\pi\sqrt{2}}\left(\frac{H_{\rm kin}}{M_P}\right)^2. \tag{55}$$

For the typical values of $H_{\rm kin}$ in Table I (and assuming $\varepsilon \simeq 0.05$), we get

$$\Theta \gtrsim 10^{-17}\left(\frac{H_{\rm kin}}{10^{11}\ {\rm GeV}}\right)^2. \tag{56}$$

Using Eq. (46), this translates into a lower bound on the radiation temperature,

$$(g_*^{\rm rad})^{1/4}T_{\rm rad} \geq 225\ {\rm GeV}. \tag{57}$$

VI. HEATING

Among the different heating mechanisms that have been proposed in the literature (see, for instance, Refs. [3,22,38–44]), there are two that can be naturally realized in a variable gravity framework: heating via gravitational interactions and heating via matter couplings involving strong adiabaticity violations. In the following, we will estimate the contribution of these heating scenarios to the heating efficiency (43) and the associated radiation temperature (44).

A. Heating via gravitational interactions

The simplest and most minimalistic heating mechanism is particle creation via gravitational interactions [4,45,46]. *Scalar* fields nonconformally coupled to the metric tensor are inevitably produced in an expanding background,[2] provided that they are light enough as compared to the Hubble rate. In our scenario, the scalar sector contains the Higgs doublet and the cosmon, but it can also include additional scalars as those appearing in extensions of the Standard Model such as grand unification.

During a Hubble time, the gravitationally induced variation of the (relativistic) scalar energy density $\Delta\rho_{\rm r}\sim T_H^4$ is associated to an effective (Hawking) temperature $T_H=H/(2\pi)$. This effect has to compete with the dilution due to the expansion of the Universe, $\rho_{\rm r}\sim a^{-4}$. During kinetic domination, $H\sim a^{-3}$ and $\Delta\rho_{\rm r}\sim a^{-12}$. In consequence, gravitational particle production is dominated by times close to the onset of the kinetic epoch, while later particle production becomes negligible. On the other hand, during the inflationary epoch, H is almost constant, and $\Delta\rho_r\sim\exp(-4N)$, with N the numbers of e-folds. Particle creation during the early stages of inflation is therefore exponentially diluted and can be also neglected. We conclude that sizable entropy production due to gravitational interactions concerns only the epoch immediately after inflation.

As seen in Fig. 4, the kinetic dominated era starts soon after the end of inflation. The energy scale of the relativistic scalars created at the onset of this regime is of order

$$T_{\rm kin}=\delta\times\frac{H_{\rm kin}}{2\pi}, \tag{58}$$

with $H_{\rm kin}^2=\rho_p^{\rm kin}/(3M_P^2)$ and $\delta\sim\mathcal{O}(1)$ an efficiency parameter [4,45]. Taking this expression into account, Eq. (43) becomes

$$\Theta=\frac{\delta^4 g_*^{\rm kin}}{1440\pi^2}\left(\frac{H_{\rm kin}}{M_P}\right)^2=10^{-19}\delta^4 g_*^{\rm kin}\left(\frac{H_{\rm kin}}{10^{11}\ {\rm GeV}}\right)^2, \tag{59}$$

resulting in a radiation temperature,

$$T_{\rm rad}=\frac{\delta^3}{24\pi^2}\sqrt{\frac{g_*^{\rm kin}}{10}}\left(\frac{g_*^{\rm kin}}{g_*^{\rm rad}}\right)^{1/4}\frac{H_{\rm kin}^2}{M_P}, \tag{60}$$

with $g_*^{\rm kin}$ the effective number of (scalar) relativistic degrees of freedom at the transition from inflation to the kinetic epoch.

If the created scalar particles are allowed to interact after production via nongravitational interactions,[3] they will rapidly generate a thermalized plasma that should contain, at least, the Standard Model degrees of freedom. In that case, the radiation temperature $T_{\rm rad}$ can be associated to the heating temperature. The effects of partial thermalization can be incorporated into a modification of the efficiency parameter δ.

Note that, although $T_{\rm rad}$ is typically above the BBN temperature $T_{\rm BBN}\simeq 0.5$ MeV, it is not high enough to satisfy the bound (56) for a moderate number of scalar fields. Indeed, combining Eqs. (55) and (59) (and assuming $\varepsilon\simeq 0.05$), we get

$$\delta^4 g_*^{\rm kin}\gtrsim\mathcal{O}(10^2). \tag{61}$$

Thus, even for $\mathcal{O}(1)$ efficiency, a large number of scalar fields is required in order to satisfy the GW constraints.

Independently of the plausibility of Eq. (61), gravitational particle production should not be considered a completely satisfactory heating mechanism. As argued in Ref. [47], the presence of light fields *during inflation* could give rise to unwanted effects, such as the generation of secondary inflationary periods or the production of large isocurvature perturbations. As we will show in the next section, these problems, together with the inefficiency of gravitational particle production, can be easily solved in the presence of *direct* couplings between the cosmon field and matter.

B. Heating via matter interactions

After Weyl rescaling, the coefficients in the quadratic part of the effective action for matter fields generically depend on ϕ (see Ref. [48] for the Higgs doublet). For a scalar field h, this dependence can be parametrized as

[2]Note, however, that this mechanism does not apply to gauge bosons and chiral fermions since their evolution equations in a conformally flat geometry as Friedmann-Robertson-Walker are invariant under Weyl rescalings.

[3]Note that this does not apply to gravitational waves, which cannot thermalize below the Planck scale [37].

$$\frac{\mathcal{L}_{\rm I}}{\sqrt{-g}} = -\frac{1}{2}[(\partial h)^2 + \gamma(\phi)(\partial h^2 \partial\phi) + M_h^2(\phi)h^2]. \quad (62)$$

The ϕ-dependence of the effective action induces particle production if the coefficients $M_h^2(\phi)$ or $\gamma(\phi)$ change substantially with time. Rapid variations of these functions are expected to occur during the crossover, where the dimensionless couplings and mass ratios of matter fields must evolve from their UV fixed-point values to those associated to the IR fixed point.[4]

To understand how a change in the effective couplings translates into particle production, let us consider the Einstein-frame equation of motion for the h-field,

$$(-\nabla^\mu\nabla_\mu + M_h^2(\phi))h = \nu(\phi)h, \quad (63)$$

with

$$\nu(\phi) = g^{\mu\nu}\nabla_\mu[\gamma(\phi)\partial_\nu\phi]. \quad (64)$$

For $\gamma(\phi) \neq 0$, the field equation for h contains derivative interactions. For the sake of simplicity, we will neglect this coupling in the following considerations and set $\gamma(\phi) = 0$.[5] For a homogeneous cosmon field [$\phi = \phi(t)$], the mode equation in Fourier space reads

$$\ddot{h}_k + 3H\dot{h}_k + \left(\frac{k^2}{a^2} + M_h^2\right)h_k = 0. \quad (65)$$

The friction term in this expression can be eliminated by performing a field redefinition $h \to a^{-3/2}h$. Doing this, we get a time-dependent harmonic oscillator equation,

$$\ddot{h}_k + \omega_k^2(t)h_k = 0, \quad (66)$$

with

$$\omega_k^2(t) = \frac{k^2}{a(t)^2} + M_h^2(t) + \Delta_a, \quad (67)$$

and

$$\Delta_a = -\frac{3}{4}\frac{\dot{a}^2}{a^2} - \frac{3}{2}\frac{\ddot{a}}{a}. \quad (68)$$

The term Δ_a is responsible for the gravitational particle production discussed in Sec. VI B. In the presence of direct couplings between the inflaton and matter fields, this term is expected to be subdominant, and it will be neglected in what follows.

The solutions of the mode equation (66) could be used to compute the propagator for the h-field in the time-dependent background $\phi(t)$, along the lines of Ref. [51]. From this, particle creation can be directly extracted. We will follow here the more conventional approach based on the operator formalism.

Let us describe the solutions of the mode equation (66) in terms of positive- and negative-frequency adiabatic solutions $\sim\exp(\pm i\int_0^t dt'\omega_k(t'))$, namely

$$h_k(t) = \frac{1}{\sqrt{2\omega_k}}[A_k(t) + B_k(t)], \quad (69)$$

with

$$A_k(t) \equiv \alpha_k(t)e^{-i\int_0^t dt'\omega_k(t')}, \quad (70)$$

$$B_k(t) \equiv \beta_k(t)e^{i\int_0^t dt'\omega_k(t')}. \quad (71)$$

The time dependence of the functions $\alpha_k(t)$ and $\beta_k(t)$ has to ensure that the mode equation (66) is obeyed. We will require $\alpha_k(t)$ and $\beta_k(t)$ to satisfy the differential equations

$$\dot{\alpha}_k(t) = \frac{\dot{\omega}_k}{2\omega_k}e^{2i\int_0^t dt'\omega_k(t')}\beta_k(t), \quad (72)$$

$$\dot{\beta}_k(t) = \frac{\dot{\omega}_k}{2\omega_k}e^{-2i\int_0^t dt'\omega_k(t')}\alpha_k(t). \quad (73)$$

These conditions induce the following evolution equations for $A_k(t)$ and $B_k(t)$:

$$\dot{A}_k(t) = \frac{\dot{\omega}_k}{2\omega_k}B_k(t) - i\omega_k A_k(t), \quad (74)$$

$$\dot{B}_k(t) = \frac{\dot{\omega}_k}{2\omega_k}A_k(t) + i\omega_k B_k(t). \quad (75)$$

The insertion of these equations into Eq. (69) yields indeed the mode equation (66).

By virtue of Eqs. (72) and (73), one obtains the conservation equation

$$\partial_t(|\alpha_k(t)|^2 - |\beta_k(t)|^2) = 0. \quad (76)$$

In particular, the Wronskian condition

$$|\alpha_k(t)|^2 - |\beta_k(t)|^2 = 1 \quad (77)$$

is preserved in time. The condition (77) arises in the operator formalism from the commutation relations of creation and annihilation operators for free fields. Extracting the propagator as the inverse of the second functional derivative of the

[4]In the Einstein frame, the matter fields must eventually decouple from the cosmon to avoid violations of the equivalence principle [27,49]. This is realized if an IR fixed point is approached.

[5]Derivative interactions give rise to similar particle production effects; see, for instance, Ref. [50].

effective action, this condition is induced by the inhomogeneous term in the propagator equation [51].

The occupation number of particles at time t can be identified with

$$n_k = |B_k(t)|^2. \tag{78}$$

The number and energy density of the created particles is therefore given by

$$n_h(t) = \frac{1}{a^3(t)} \int \frac{d^3k}{(2\pi)^3} n_k, \tag{79}$$

$$\rho_h(t) = \frac{1}{a^3(t)} \int \frac{d^3k}{(2\pi)^3} \omega_k n_k. \tag{80}$$

Using

$$\dot{h}_k(t) = -i\sqrt{\frac{\omega_k}{2}}(A_k(t) - B_k(t)), \tag{81}$$

one infers the relation

$$|A_k(t)|^2 + |B_k(t)|^2 = \frac{1}{\omega_k}|\dot{h}_k(t)|^2 + \omega_k |h_k(t)|^2. \tag{82}$$

This, together with the condition $|A_k|^2 - |B_k|^2 = 1$, translates for the occupation numbers to

$$n_k = \frac{1}{2\omega_k}(|\dot{h}_k|^2 + \omega_k^2 |h_k|^2) - \frac{1}{2}. \tag{83}$$

Vacuum initial conditions correspond to $\alpha_k(t_{\rm init}) = 1$ and $\beta_k(t_{\rm init}) = 0$ and therefore to $n_k(t_{\rm init}) = 0$. In terms of h_k, these initial conditions become

$$h_k(t \to t_{\rm init}) = \frac{1}{\sqrt{2\omega_k(t)}} e^{-i\int_0^t dt' \omega_k(t')}. \tag{84}$$

For particle production to be efficient, the adiabaticity condition $|\dot{\omega}_k| \ll \omega_k^2$ must be significantly violated [52], as clearly visible in Eq. (75). The energy density of the produced particles obeys

$$(\partial_t + 3H)\rho_h = \frac{1}{2a^3} \int \frac{d^3k}{(2\pi^3)} \dot{\omega}_k (2\omega_k |h_k|^2 - 1).$$

The production term on the right-hand side is indeed proportional to $\dot{\omega}_k$. It has to compete with the Hubble damping on the left-hand side.

In the absence of derivative interactions [i.e., for $\gamma(\phi) = 0$ in Eq. (62)], the cosmon field ϕ couples to the matter field h only through the effective mass function $M_h^2(\phi)$. In a natural and phenomenologically successful scenario, this function should satisfy the following criteria:

(i) It should be large enough during inflation to retain the single-field inflationary picture and avoid the generation of large isocurvature perturbations.
(ii) It should rapidly vary at the end of inflation ($\phi \gtrsim \phi_{\rm end}$) to heat the Universe via violations of the adiabaticity condition $|\dot{\omega}_k| \ll \omega_k^2$.
(iii) It should eventually become independent of ϕ if the field h is the Higgs doublet. This reflects scale symmetry in the Standard Model sector as required by the bounds on the variation of the ratio of the Fermi scale over the Planck scale since nucleosynthesis.

We assume here that the crossover from the UV to the IR fixed point, which is reflected in the change of the cosmon kinetic term and associated to the end of inflation, leaves also its traces in the matter sector. In the field range $\chi \approx m$, the couplings of h to χ, and correspondingly to ϕ, are therefore expected to undergo significant changes. This provides for a natural scenario where $M_h^2(\phi)$ can change rapidly from large to small values at the end of inflation. The conditions i–iii can be viewed as the imprint of the crossover in the matter sector.

C. Workout example

A possible parametrization of $M_h^2(\phi)$ satisfying the above requirements is $M_h^2(\phi) \equiv \epsilon(\phi) M_P^2$ with

$$\epsilon(\phi) = \epsilon_\infty + \epsilon_1 \left[\frac{\exp(-Y_\epsilon(\phi))}{Y_\epsilon(\phi)}\right]^{\sigma_h/2}. \tag{85}$$

Here,

$$Y_\epsilon(\phi) = 1 + \frac{1}{2}\left[\frac{\phi^2}{\phi_\epsilon^2} + \frac{\phi}{\phi_\epsilon}\sqrt{4 + \frac{\phi^2}{\phi_\epsilon^2}}\right], \tag{86}$$

and σ_h, ϵ_∞, ϵ_1, and ϕ_ϵ are taken to be positive constants. The shape of $\epsilon(\phi) - \epsilon_\infty$ mimics the form of the cosmon potential (15), with σ_h, ϕ_ϵ, and the amplitude ϵ_1 left free. The detailed structure of this parametrization is chosen for illustration purposes only. Alternative choices sharing the features described in i, ii, and iii could be used without modifying the conclusions below.

The behavior of Eq. (85) for different values of ϕ_ϵ is shown in Fig. 5. It describes the evolution from a UV fixed point,[6]

$$\phi \partial_\phi \epsilon(\phi) \approx \sigma_h \epsilon(\phi)(1 - \phi_\epsilon^2/\phi^2), \tag{88}$$

[6]In the far UV ($\phi \gg \phi_t, \phi_\epsilon$), this corresponds in the scaling frame to a flow equation,

$$\mu \partial_\mu \epsilon(\chi) \approx \bar{\sigma}_h \epsilon(\chi), \tag{87}$$

with $\bar{\sigma}_h = \sigma_h \sigma/2$.

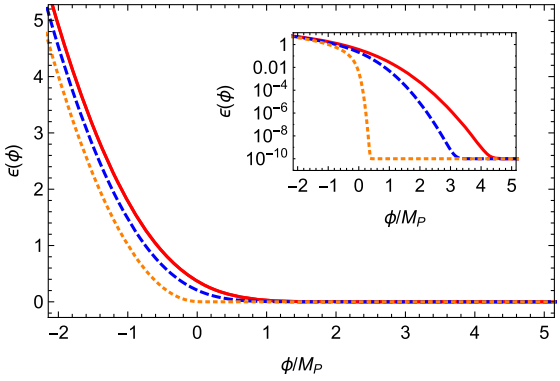

FIG. 5. The effective coupling $\epsilon(\phi)$ for $\sigma_h = 2$, $\epsilon_\infty = 10^{-10}$, $\epsilon_1 M_P^2 = \phi_\epsilon^2$, and different values of ϕ_ϵ. All cases share the same asymptotic behavior during inflation. The red-solid, blue-dashed, and orange-dotted lines correspond respectively to $\phi_\epsilon = M_P, 0.75 M_P$, and $10^{-1} M_P$. In the inset, we plot $\epsilon(\phi)$ logarithmically in order to better resolve the approach to zero and to facilitate the comparison with Fig. 2.

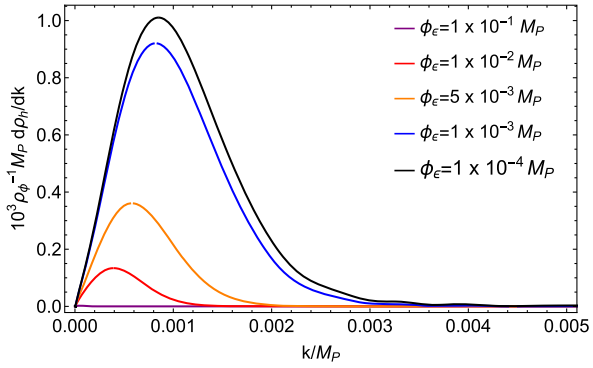

FIG. 6. The spectra of produced h particles for $\sigma_h = 2$, $\epsilon_\infty = 10^{-10}$, $\epsilon_1 = 10^{-1}\phi_\epsilon^2/M_P^2$, and different choices of ϕ_ϵ. All cases are evaluated at the onset of the kinetic domination regime. At that time, $H_{\rm kin} \simeq 1.63 \times 10^{11}$ GeV, and $\rho_\phi^{\rm kin} \simeq (8.4 \times 10^{14}\ {\rm GeV})^4$.

approached for $\phi \to -\infty$ with anomalous dimension σ_h, to an IR fixed point where $\epsilon \approx \epsilon_\infty$. The constant ϕ_ϵ encodes the location of the transition. The smaller the value of ϕ_ϵ, the longer the effective coupling stays in the vicinity of the UV fixed point.

For large values of ϕ_ϵ, we can make use of Eq. (35) to relate this parameter to the crossover scale m signaling the end of inflation,

$$\frac{\chi_\epsilon}{m} = \left(\frac{\kappa}{\sigma}\frac{\phi_t^2}{\phi_\epsilon^2}\right)^{1/\sigma}. \tag{89}$$

Values of ϕ_ϵ^2 larger than ϕ_t^2 correspond to values of χ_ϵ smaller than the crossover scale m. For $\phi_\epsilon/\phi_t \ll 1$, the transition in $M_h(\phi)$ occurs within a short period before the end of inflation. In this region, the size of ϕ_ϵ mainly determines the sharpness of the crossover, with small ϕ_ϵ leading to a more abrupt transition. We could introduce and additional parameter ϕ_l for the *timing* of the transition, e.g., by replacing ϕ in Eq. (85) by $\phi - \phi_l$. All our models can account for a gauge hierarchy if $\epsilon_\infty \ll 1$ with $\epsilon \gtrsim 1$ for $\phi \to -\infty$ ($\chi \to 0$) and $\epsilon \to \epsilon_\infty$ for $\phi \to \infty$ ($\chi \to \infty$).

The occupation numbers and the energy density of created particles for a given set of parameters $(\sigma_h, \epsilon_\infty, \epsilon_1, \phi_\epsilon)$ can be computed by numerically solving the mode equation (66) with vacuum initial conditions. Let us consider for concreteness an anomalous dimension $\sigma_h = 2$ in an inflationary model with $\sigma = 4$ and $\kappa = 1$. For this choice of parameters, the interaction Lagrangian during inflation ($\phi \ll -\phi_\epsilon$) contains a quartic term $-(1/2)g^2\phi^2h^2$ with $g^2 \equiv \epsilon_1 M_P^2/\phi_\epsilon^2$. To retain the predictions of single-field inflation, we will require the effective mass $g|\phi|$ of the scalar field h during inflation to be larger than the mass of the cosmon. In the leading order approximation (24), the squared cosmon mass $M_c^2 \equiv M_P^4 \partial^2 V/\partial\phi^2$ reads

$$M_c^2 = \frac{4A(4-\sigma)}{\sigma^2}\left(\frac{\phi^2}{M_P^2}\right)^{\frac{2}{\sigma}-1} M_P^2. \tag{90}$$

This expression vanishes for $\sigma = 4$ and is generically suppressed by the small factor A, cf. Eqs. (25) and (33). Unless g is tiny, the effective mass of the h field during inflation will be significantly larger than the cosmon mass. For our practical example, we choose $g^2 = 0.1$, while keeping ϕ_ϵ as a free parameter. For ϵ_∞, we take $\epsilon_\infty = 10^{-10}$, which translates into an asymptotic h mass of order $\epsilon_\infty^{1/2} M_P \simeq \mathcal{O}(10^{13}\ {\rm GeV})$ at $\phi \to \infty$. Smaller values of ϵ_∞, as those required if h is the Higgs doublet, will not change our discussion.

The numerical results for different values of ϕ_ϵ are summarized in Fig. 6 and Table II. All cases are evaluated at the onset of the kinetic domination regime. At that time, $H_{\rm kin} \simeq 1.63 \times 10^{11}$ GeV, and $\rho_\phi^{\rm kin} \simeq (8.4 \times 10^{14}\ {\rm GeV})^4$. In agreement with the analytical estimates presented in Appendix B, smaller choices of ϕ_ϵ translate into more significant particle production.

TABLE II. Heating efficiency Θ, as defined by the ratio (43) between the radiation and cosmon energy densities at the onset of kinetic domination and the associated radiation temperature (44) for different values of ϕ_ϵ. Parameters are taken as $\sigma_h = 2$, $\epsilon_\infty = 10^{-10}$, and $\epsilon_1 = 10^{-1}\phi_\epsilon^2/M_P^2$. At the onset of kinetic domination, one has $H_{\rm kin} \simeq 1.63 \times 10^{11}$ GeV and $\rho_\phi^{\rm kin} \simeq (8.4 \times 10^{14}\ {\rm GeV})^4$.

ϕ_ϵ/M_P	Θ	$(g_*^{\rm rad})^{\frac{1}{4}} T_{\rm rad}$ (GeV)
1×10^{-1}	2.5×10^{-9}	3.9×10^{8}
1×10^{-2}	9.7×10^{-8}	6.1×10^{9}
5×10^{-3}	3.3×10^{-7}	1.5×10^{10}
1×10^{-3}	1.2×10^{-6}	4.0×10^{10}
1×10^{-4}	1.4×10^{-6}	4.4×10^{10}

The energy density of the produced particles can be compared with the energy density of the cosmon at the onset of radiation domination. The resulting heating efficiency (43) determines the radiation temperature $T_{\rm rad}$ via Eq. (44). As shown in Table II, this temperature is well above the BBN temperature ($T_{\rm BBN} \simeq 0.5$ MeV) and significantly exceeds the energy scale associated to gravitational particle production. Note also that the GW bound (56) can be easily satisfied even if only one matter field violates the adiabaticity condition. If this condition is violated in n_a channels, the ratio (43) and the associated radiation temperature are enhanced by a factor $\Theta \to n_a\Theta$ and $T_{\rm rad} \to \sqrt{n_a} T_{\rm rad}$. Since the main aspects of particle creation due to a *single* violation of adiabaticity are independent of the spin of the particle, the above results can be extended to fermionic species [53,54].

We finish this section by noticing that the heating scenario presented here is conceptually different from the *instant reheating* mechanisms [47,55] appearing in most quintessential inflation models [22,39,40]. Instant reheating is usually formulated in terms of ϕ-symmetric interactions among the inflaton field ϕ and some scalar particle X which is itself coupled to fermions via Yukawa interactions,

$$\frac{\mathcal{L}_{\rm I}}{\sqrt{-g}} = -\frac{1}{2} g^2 \phi^2 X^2 - y_\psi X \bar{\psi}\psi. \tag{91}$$

As in our case, a small fraction of X particles is automatically generated at the end of inflation via the violation of the adiabaticity condition at $\phi \approx 0$. After particle production, the inflaton field rolls down the quintessence potential (15). This rolling increases the effective mass of the X field ($m_X(\phi) = g|\phi|$) and amplifies its energy density and the probability to decay into fermions [$\Gamma_{X\to\bar{\psi}\psi} \propto m_X(\phi)$]. As argued in Ref. [47], to avoid significant backreaction effects into the inflaton evolution equation

$$\ddot{\phi} + 3H\dot{\phi} + V_{,\phi} = -g^2\phi\langle X\rangle^2, \tag{92}$$

the decay into fermions should take place soon after particle production. This requirement translates into a mild condition relating the couplings y_t and g^2 [47].

Although instant reheating is a highly efficient mechanism that could give rise to radiation temperatures well above those displayed in Table II, we find it difficult to implement in a variable gravity scenario like the one under consideration. For a simple crossover, a monotonic dependence of $M_h^2(\phi)$ on ϕ seems more natural. We emphasize that an *instant feeding* of the created particles is not necessary in our scenario. If the fraction of energy depleted out of the cosmon component exceeds the GW bound (56), the Universe will become safely dominated by radiation before BBN. Our scenario does not suffer from backreaction problems since the mass of the h-field is a monotonically decreasing function of the inflaton field ϕ.

VII. HOT BIG BANG ERA

In the Einstein frame, the evolution during the hot big bang era can be described in terms of the Friedmann equations and the Klein-Gordon equation for the cosmon field,

$$H^2 = \frac{1}{3M_P^2}(\rho_\phi + \rho_R + \rho_M), \tag{93}$$

$$\dot{H} = -\frac{1}{2M_P^2}\left(\dot{\phi}^2 + \frac{4}{3}\rho_R + \rho_M\right), \tag{94}$$

$$\ddot{\phi} + 3H\dot{\phi} + M_P^4 V_{,\phi} = 0, \tag{95}$$

with $\rho_\phi = \dot{\phi}^2/2 + M_P^4 V$ and ρ_R and ρ_M the energy densities of radiation and nonrelativistic matter with conservation equations

$$\dot{\rho}_R + 4H\rho_R = 0, \qquad \dot{\rho}_M + 3H\rho_M = 0. \tag{96}$$

A. Onset of radiation domination

The evolution of the dark energy equation of state $w_\phi = p_\phi/\rho_\phi$ and the (normalized) energy densities $\Omega_i \equiv \rho_i/(3M_P^2H^2)$ with $i = \phi, R$, and M can be obtained by numerically solving the cosmological equations (93)–(96). We assume a number of production channels of the order of the number of degrees of freedom in the Standard Model, $\mathcal{O}(10^2)$. The results for $\sigma = 4$, $\kappa = 1$, and $\Theta = 10^{-4}$ are shown in Figs. 7, 8, and 9. The qualitative behavior of the observables in these figures can be understood as follows:

(a) At the end of inflation, the radiation component Ω_R is very small, $\Omega_R \sim \Theta$. The cosmon evolution is

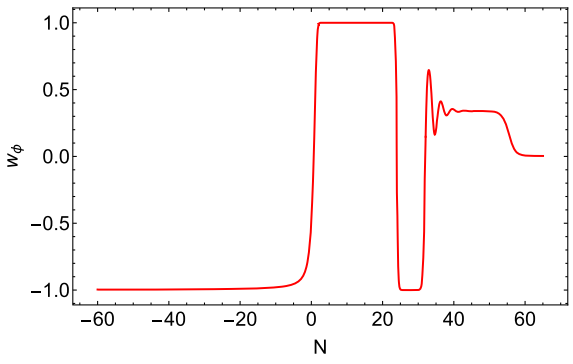

FIG. 7. Evolution of the dark energy equation of state $w_\phi = p_\phi/\rho_\phi$ from the inflationary era to the matter dominated era as a function of the number of e-folds. The end of inflation corresponds to $N = 0$. For this plot, we chose $\sigma = 4$, $\kappa = 1$ and assumed a heating efficiency $\Theta = 10^{-4}$.

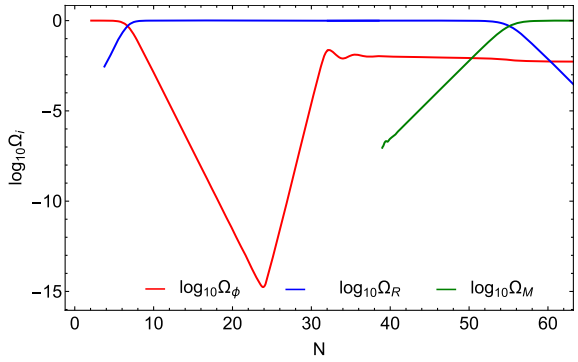

FIG. 8. Postinflationary evolution of the density parameters Ω_ϕ, Ω_R, and Ω_M as a function of the number of e-folds. The end of inflation corresponds to $N = 0$. Parameters are chosen as in Fig. 7.

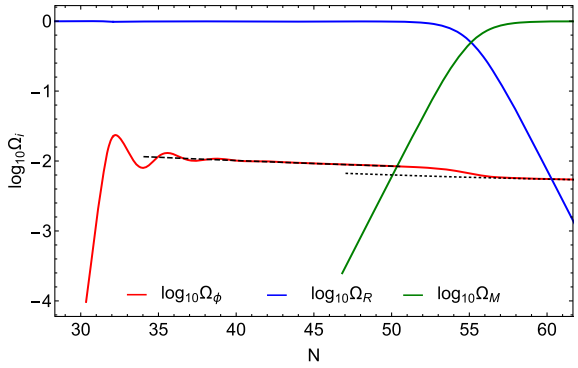

FIG. 9. Detailed view of the density parameters Ω_R, Ω_M, and Ω_ϕ during matter and radiation domination as a function of the number of e-folds using the same parameters in Fig. 7. The expression (112) with $n = 4$ and $n = 3$ is depicted with black dashed lines. Nucleosynthesis corresponds to $N \simeq 41$.

dominated by its kinetic energy density. This domination is reflected in the dark energy equation-of-state parameter w_ϕ, which is close to 1 for the kinetic epoch. The rapid rolling of the cosmon field down the quintessence potential translates into a substantial decrease of $V(\phi)$. Once ρ_R becomes comparable with ρ_ϕ, a rapid decrease of the density parameter Ω_ϕ takes place.

(b) When ρ_R become dominant, the Hubble parameter changes its behavior to $H = 1/(2t)$. As long as the kinetic energy of the cosmon dominates over the potential energy, $\ddot{\phi} + 3H\dot{\phi} \simeq 0$, the evolution (39) switches to

$$\phi(t) = \phi_{\rm rad} + 2\dot{\phi}_{\rm rad} t_{\rm rad}\left(1 - \sqrt{\frac{t_{\rm rad}}{t}}\right), \qquad (97)$$

with $\phi_{\rm rad}$ and $\dot{\phi}_{\rm rad}$ the value of the field and its velocity at the onset of radiation domination $t_{\rm rad}$. For $t \gg t_{\rm rad}$, the field approaches the constant value $\phi_{\rm f} \simeq \phi_{\rm rad} + 2\dot{\phi}_{\rm rad} t_{\rm rad}$. This *freezing* of the cosmon field translates into a substantial decrease of the cosmon kinetic energy density and an eventual resurgence of the potential counterpart, which is, however, subdominant with respect to the radiation component. During this period, the equation-of-state parameter approaches $w_\phi \simeq -1$, and the dark energy fraction Ω_ϕ starts to grow.

(c) Once ρ_ϕ approaches ρ_R again, the evolution settles to a scaling or tracker solution. After some oscillations, the dark energy equation of state attains a nearly constant value $w_\phi \simeq 1/3$, which evolves toward $w_\phi \simeq 0$ after matter-radiation equality. In both periods, the dark energy density parameter Ω_ϕ *tracks* the dominant energy component.

B. Heating efficiency

The details of the heating process are not important for observational consequences. The only thing relevant is that the heating terminates before the end of the kination epoch. We can then use the ratio of energy densities in radiation and the scalar field at any moment after the end of the heating process in order to give a generalized definition of the heating efficiency Θ. During the early stages of the kinetic epoch, the radiation energy density is so small that it does not influence the cosmological evolution. For instant particle production, we can compute ρ_R/ρ_ϕ at any given time during this period in terms of the scaling efficiency Θ in Eq. (43),

$$\frac{\rho_R(a)}{\rho_\phi(a)} = \Theta\left(\frac{a}{a_{\rm kin}}\right)^2. \qquad (98)$$

We can employ this expression as a practical definition of Θ for scenarios with an extended heating period. For any time or scale factor a in the region where the heating is not efficient any longer, but radiation is still subdominant, the heating efficiency can be defined by the radiation fraction at that moment multiplied by $(a_{\rm kin}/a)^2$. Defined in this way, the parameter Θ is sufficient for the description of the later evolution. The details of the heating process beyond the determination of Θ are not needed in practice.

In particular, we can use Eq. (98) at the beginning of radiation domination $a = a_{\rm rad}$, where $\rho_\phi(a_{\rm rad}) = \rho_R(a_{\rm rad})$ and

$$\left(\frac{a_{\rm kin}}{a_{\rm rad}}\right)^2 = \Theta. \qquad (99)$$

Given a heating efficiency, the number of e-folds needed to explain the approximate flatness and homogeneity of the observable Universe is completely determined. The horizon crossing of the pivot scale $k_{\rm hc}$ is defined as

$$k_{\rm hc} = a_{\rm hc} H_{\rm hc} = a_{\rm end} e^{-N(k_{\rm hc})} H_{\rm hc}, \tag{100}$$

with $N(k_{\rm hc})$ the number of e-folds before the end of inflation. Assuming the kinetic regime to start immediately after the end of inflation ($a_{\rm end} \simeq a_{\rm kin}$, $\rho_{\rm end} \simeq \rho_{\rm kin}$) and taking into account the scaling of the different energy components, we can rewrite Eq. (100) as

$$\begin{aligned} N = &-\ln\left(\frac{k_{\rm hc}}{a_0 H_0}\right) \\ &+ \ln\left(\frac{H_{\rm hc}}{H_0}\right) + \frac{1}{4}\ln\left(\frac{\rho_{\rm mat}}{\rho_{\rm hc}}\right) + \ln\left(\frac{a_{\rm mat}}{a_0}\right) \\ &- \frac{1}{2}\ln\left(\frac{a_{\rm kin}}{a_{\rm rad}}\right) + \frac{1}{4}\ln\left(\frac{\rho_{\rm hc}}{\rho_{\rm kin}}\right), \end{aligned} \tag{101}$$

where the subindices kin, rad, mat, and 0 denote respectively the onset of kinetic, radiation, and matter dominated eras and the present cosmological epoch. Equation (101) is universal and valid for any inflationary potential. The precise shape of the potential is needed to relate the energy density at the end of inflation ($\rho_{\rm end} \simeq \rho_{\rm kin}$) to the energy density at horizon crossing ($\rho_{\rm hc}$). Neglecting the small energy density variation between these two epochs ($\rho_{\rm hc} \simeq \rho_{\rm end} \simeq \rho_{\rm kin}$), we can approximate Eq. (101) by ($a_0 = 1$)

$$\begin{aligned} N \simeq &-\ln\left(\frac{k_{\rm hc}}{T_0}\right) + \frac{1}{4}\ln\left(\frac{\pi^2 g_{\rm mat} \mathcal{A}}{135}\right) \\ &+ \frac{1}{4}\ln r - \frac{1}{4}\ln\Theta, \end{aligned} \tag{102}$$

where we have made use of Eqs. (32) and (99) together with the standard relations

$$\rho_{\rm mat} \simeq \frac{\pi^2 g_{\rm mat}}{15} T_{\rm mat}^4, \qquad \frac{a_{\rm mat}}{a_0} = \frac{T_0}{T_{\rm mat}}. \tag{103}$$

Here, $g_{\rm mat} = 3.36$ stands for the number of relativistic degrees of freedom at matter-radiation equality.

Taking into account the pivot scale $k_{\rm hc} = 0.002\,{\rm Mpc}^{-1} = 1.27 \times 10^{-32}\,{\rm eV}$ used in the derivation of the *combined* Planck/BICEP2 results [32,33], Eq. (102) becomes[7]

$$N \simeq 62 + \frac{1}{4}\ln\left(\frac{r}{0.05}\right) - \frac{1}{4}\ln\left(\frac{\Theta}{10^{-4}}\right). \tag{104}$$

The behavior of the number of e-folds as a function of the heating efficiency Θ is shown in Fig. 10. As clearly appreciated in this figure, our highly efficient heating scenario translates into a rapid onset of radiation domination and into a number of e-folds rather close to the standard value $N \sim 60$.

[7]We use $T_0 \simeq 2.73{\rm K} \simeq 2.35 \times 10^{-4}$ eV.

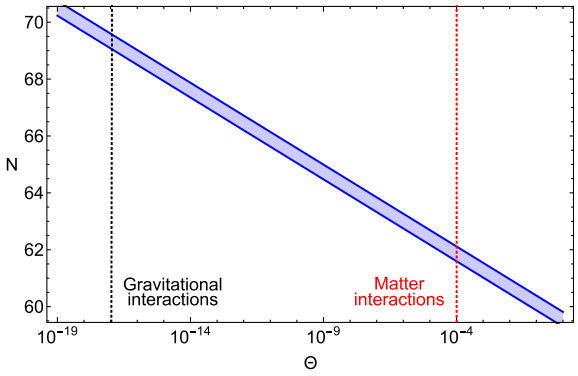

FIG. 10. The number of e-folds (104) as a function of the heating efficiency Θ. The blue region stands for variations of the tensor-to-scalar ratio r within the range [0.01, 0.08]. The vertical lines indicate the typical values of the heating efficiency associated to gravitational and matter interactions. For these lines, we assume a number of production channels of the order of the number of degrees of freedom in the Standard Model, $\mathcal{O}(10^2)$ [cf. Eq. (59) and Table II]. Enhanced particle contents as those appearing in Standard Model extensions such as grand unification would translate into a larger heating efficiency and therefore into a smaller number of e-folds N.

C. Scaling solution

During the radiation dominated epoch, the dark energy density decreases according to a scaling solution [1]. The behavior of the scaling solution can be easily understood by considering the evolution equations for the cosmological observables during matter and radiation domination in terms of suitable variables. For $\rho = \rho_R + \rho_M$, $\dot{\rho} + nH\dot{\rho} = 0$, and constant n ($n = 4$ for radiation domination, $n = 3$ for matter domination), one has [49,56,57]

$$\frac{w_\phi'}{1 - w_\phi} = -3(1 + w_\phi) + \lambda\sqrt{3(1 + w_\phi)\Omega_\phi}, \tag{105}$$

$$\Omega_\phi' = -\Omega_\phi(1 - \Omega_\phi)(3(1 + w_\phi) - n), \tag{106}$$

$$\lambda' = -\sqrt{3(1 + w_\phi)\Omega_\phi}(\Gamma - 1)\lambda^2, \tag{107}$$

where the primes denote derivatives with respect to the number of e-folds. The slow-roll parameters

$$\lambda \equiv -M_{\rm P}\frac{V_{,\phi}}{V}, \qquad \Gamma \equiv \frac{V V_{,\phi\phi}}{V_{,\phi}^2} \tag{108}$$

characterize the slope and curvature of the quintessence cosmon potential.

A simple inspection of Eqs. (105) and (106) reveals for constant λ a fixed point at

$$\Omega_\phi = \frac{n}{\lambda}, \qquad w_\phi = \frac{n - 3}{3}. \tag{109}$$

This case corresponds to an exponential potential, for which a *scaling* or *tracker* solution is well known to exist and to be stable [1,2,18,58].

For the potential (15), the slow-roll parameters (108) become

$$\lambda = 2\sqrt{\frac{\kappa Y}{\sigma}}, \qquad \Gamma = 1 - \frac{\sigma}{4(1+Y)}, \tag{110}$$

with Y given by Eq. (16). Combining these expressions, we obtain a relation between Γ and λ,

$$\Gamma(\lambda) = 1 - \frac{\kappa\sigma}{4\kappa + \sigma\lambda^2}, \tag{111}$$

that *closes* the system of autonomous equations (105)–(107).

Since $\Gamma \neq 1$, the λ parameter must evolve on time, cf. Eq. (107). Note, however, that at large field values ($\phi \gg \phi_t$), the function Y becomes approximately $Y \approx \phi^2/\phi_t^2 + 2 \gg 1$, which translates into a value of Γ that tends asymptotically to 1. In this limit, the relations (109) may still be considered as some *fixed trajectory* with slowly varying λ. Taking into account the first equation in (110), this asymptotic behavior can be written as

$$\Omega_\phi = \frac{n\sigma}{4\kappa Y(\phi)} = \frac{nB(\phi(\chi))}{4}, \tag{112}$$

which coincides with the approximate expression at large χ found in Ref. [19].

The relation (112) can be used to obtain bounds on κ from early dark energy constraints. Using Eq. (7), we can rewrite Eq. (112) as

$$\Omega_\phi \simeq \frac{n\sigma}{4\kappa}\mathcal{W}^{-1}\left[\left(\frac{V_0}{V}\right)^{\sigma/2}\right], \tag{113}$$

with $\mathcal{W}$ the Lambert function and V_0 given by Eq. (17), with m/μ satisfying the inflationary constraint (33). For the epoch of nucleosynthesis, we may employ $M_P^4 V \approx T_{\rm BBN}^4$. The dependence of $\Omega_\phi^{\rm BBN}$ on σ and κ is illustrated in Fig. 11 for typical values $N = 60$ and $T_{\rm BBN} = 1$ MeV. As is clearly seen in this figure, the early dark energy fraction strongly depends on κ, while it is rather insensitive to the precise value of the UV anomalous dimension σ, provided that this is not very close to zero. The current observations [33,59–61] restrict $\Omega_\phi^{\rm BBN}$ to be smaller than 2%, which can be easily satisfied for $\kappa > 0.5$.

The time when Ω_ϕ reaches the scaling solution ($N \approx 32$ in Fig. 9) depends on the heating efficiency Θ. The smaller the Θ, the later the radiation domination sets in, the smaller the V is when the evolution of the scalar field stops and therefore the later the onset of the scaling solution is. Only after the onset of the scaling solution, a non-negligible fraction of early dark energy is present. In particular, the

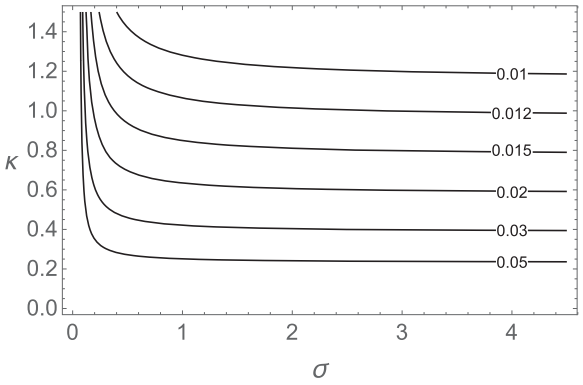

FIG. 11. The fraction of early dark energy (112) at BBN as a function of the model parameters κ and σ. For this plot, we set $T_{\rm BBN} = 1$ MeV and $w_\phi \simeq 1/3$.

BBN constraint applies only if the cosmon field reaches the attractor solution before BBN. This is not guaranteed for very long kinetic regimes, even if the GW bound in Eq. (56) is satisfied. For the particular parameters considered in this section, the attractor solution is not reached before BBN if the heating efficiency is below $\Theta \simeq 10^{-13}$. Further constraints on early dark energy arise from the detailed properties of the CMB spectrum, which depend on Ω_ϕ at the time of CMB emission. The bounds [62] are strength similar to the BBN bounds. The presence of early dark energy during structure formation reduces the presently observable structure as compared to the CMB prediction in the standard cold dark matter scenario. As a rough rule, 1% Ω_ϕ reduces σ_8 by 5% [63].

At the end of this section, we may recall that the hot big bang picture is a property of the Einstein frame. In the scaling frame, both the particle masses and the Planck scale increase with time. The Universe shrinks during radiation and matter domination eras, and the temperature of the Universe increases [19–21]. Only dimensionless ratios such as temperature over particle mass or distance between galaxies over atom size show the same behavior in both frames.

VIII. LATE DARK ENERGY DOMINATION

An exit mechanism from the scaling regime is needed in order to obtain late-time acceleration. A rather natural setup arises if the neutrino-to-electron-mass ratio increases with increasing ϕ in the present cosmological epoch [64,65]. In our scenario, this effect can be induced by a second crossover stage in the beyond the Standard Model sector, which manifests itself through the nonrenormalizable neutrino mass operator. A decrease of the mass of the right-handed neutrinos or of a heavy scalar triplet (seesaw I or II mechanism) in units of χ results in an increase of the mass ratio between the light left-handed neutrinos and the electron. More quantitatively, we may define in the scaling frame

$$\tilde{\gamma}(\chi) = \frac{1}{2}\chi\frac{\partial}{\partial\chi}\ln\frac{m_\nu(\chi)}{\chi}, \tag{114}$$

with $m_\nu(\chi)$ the average of the masses of the left-handed neutrinos. For the particular example

$$m_\nu(\chi) = \frac{c_\nu\chi}{\ln\left(\frac{\chi_0^2}{\chi^2}\right)}, \tag{115}$$

one has

$$\tilde{\gamma} = \frac{1}{\ln\left(\frac{\chi_0^2}{\chi^2}\right)}. \tag{116}$$

In the Einstein frame with fixed electron mass, only the neutrino mass depends on the cosmon field, defining the effective neutrino-cosmon coupling

$$\beta = -M_P\frac{\partial}{\partial\phi}\ln m_\nu(\phi). \tag{117}$$

A typical behavior of this quantity, corresponding to Eq. (115), is parametrized by

$$\beta = \frac{M_P}{\phi - \phi_c}. \tag{118}$$

Only finite values of $\beta \approx 100$ will occur, such that the singularity in Eq. (118) is never reached and can be removed by a different behavior at small $|\phi - \phi_c|$. The cosmon-neutrino coupling modifies the Klein-Gordon equation for the scalar field [18,66,67]

$$\ddot{\phi} + 3H\dot{\phi} = -V_{,\phi} + \frac{\beta}{M_P}(\rho_\nu - 3p_\nu) \tag{119}$$

and the conservation equation for the neutrino energy density

$$\dot{\rho}_\nu + 3H(\rho_\nu + p_\nu) = -\frac{\beta}{M_P}(\rho_\nu - 3p_\nu)\dot{\phi}. \tag{120}$$

These modifications are negligible as long as neutrinos are relativistic, $p_\nu = \rho_\nu/3$. As soon as neutrinos become nonrelativistic, a negative coupling β effectively stops the evolution of ϕ, ending the scaling solution and leading to a cosmology that looks rather close to a cosmological constant afterward. More precisely, the ratio of dark energy to neutrino energy density quickly approaches the value

$$\frac{\Omega_\phi}{\Omega_\nu} = \tilde{\gamma} = -\frac{\beta}{M_P}\left(\frac{\partial\ln V}{\partial\phi}\right)^{-1}. \tag{121}$$

Neutrinos become nonrelativistic at redshift $z_{\rm NR} \approx 5$ [68], and the present dark energy density corresponds to $\Omega_\phi\rho_c$ at $z_{\rm NR}$. The resulting relation between the present dark energy density and neutrinos involves a dimensionless parameter γ_ν for the growth rate of the neutrino mass [65],

$$\rho_\phi(t_0)^{1/4} = 1.27\left(\frac{\gamma_\nu m_\nu(t_0)}{\rm eV}\right)^{1/4}10^{-3}\ {\rm eV}, \tag{122}$$

with $\gamma_\nu = \tilde{\gamma}(t_0)$ and $m_\nu(t_0)$ the average of the present neutrino masses. This is of the same order as the observed value $\rho_\phi(t_0)^{1/4} = 2\times10^{-3}$ eV. The equation of state is close to -1,

$$w(t_0) = -1 + \frac{m_\nu(t_0)}{12\ {\rm eV}}. \tag{123}$$

For γ_ν of order 1, the scenario is rather successful for the range of neutrino masses compatible with observations. Realistic setups taking into account backreaction effects can be built on this mechanism [69].

IX. CONCLUSIONS

At the UV and IR fixed points of a variable gravity scenario, scale invariance becomes an exact symmetry of the quantum theory. Such a simple setup can remarkably give rise to inflation and dark energy using a *single* scalar field. Approximate scale symmetry near the UV fixed point manifests itself in the approximate scale invariance of the primordial fluctuation spectrum. Approximate scale symmetry near the IR fixed point produces an almost massless *cosmon field* responsible for present dynamical dark energy. In the limit of exact scale symmetry, this field becomes the massless Goldstone boson of spontaneously broken scale invariance (dilaton). A simple quadratic potential and a moderately varying kinetic term in the scaling frame produce a rich cosmological history, the sequence of epochs of which is summarized in Fig. 12.

The graviscalar sector of our model involves only a small number of dimensionless parameters of order 1: σ, κ, $c_t = \ln(m/\mu)$, and γ_ν. In particular, it explains the tiny value of the present dark energy density (in the unit of M_P) without involving any tiny or large coupling and without any tuning of couplings. If quantum gravity generates indeed an effective action of the type (1), this solves the cosmological constant problem. If, furthermore, there exists a second crossover stage leading to a growing neutrino to electron mass ratio, this solves the why now problem of dark energy. The main characteristics of our model are not taken completely *ad hoc*. They are rather directly related to general properties at the fixed points.

We derived a compact Einstein-frame formulation of the model in terms of Lambert functions and proved that it can support inflation via a power-law inflationary potential. The spectrum of primordial fluctuations turned out to depend only on the UV anomalous dimension σ, while the amplitude is set by the integration constant of the running

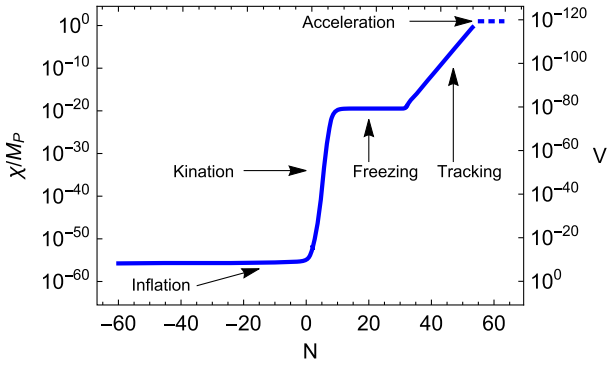

FIG. 12. Evolution of the cosmon field χ and the dimensionless cosmon potential (15) as a function of the number of e-folds. The end of inflation corresponds to $N = 0$. For this plot, we chose $\sigma = 4$, $\kappa = 1$ and assumed a heating efficiency $\Theta \simeq 10^{-4}$.

kinetic term or the ratio μ/m. The crossover to the IR fixed point manifests itself as a steep potential in the Einstein frame. This ends inflation and triggers the onset of a kinetic domination regime. By considering two natural heating scenarios within the variable gravity framework, we showed that this kination era is limited in time. The cosmologically relevant properties of the heating process can be summarized in a single parameter, the heating efficiency Θ. Kinetic domination is naturally followed by a standard hot big bang era, where the (subdominant) dark energy component tracks the (dominant) radiation/matter content. By comparing this tracking solution with early dark energy constraints, we derived a lower bound on the IR parameter κ. The end of the scaling behavior and the beginning of the present accelerated expansion of the Universe can be induced by an additional crossover in sectors beyond the Standard Model. This determines the last free parameter γ_ν related to the present growth rate of the neutrino mass.

With all parameters determined or constrained by present observations, our model is rather predictive. We will see if its simplest form can survive the next round of cosmological tests.

ACKNOWLEDGMENTS

We acknowledge support from ERC-AdG-290623 and from DFG through the project TRR33 "The Dark Universe."

APPENDIX A: THE LAMBERT FUNCTION

The Lambert function $\mathcal{W}$ [30] is defined as the inverse of the function $f(\tilde{x}) = \tilde{x}e^{\tilde{x}}$, i.e.,

$$\tilde{x} = f^{-1}(\tilde{x}e^{\tilde{x}}) = \mathcal{W}(\tilde{x}e^{\tilde{x}}). \tag{A1}$$

Substituting $x = \tilde{x}e^{\tilde{x}}$ in this expression, we obtain the defining equation for $\mathcal{W}(x)$,

$$x = \mathcal{W}(x)e^{\mathcal{W}(x)}. \tag{A2}$$

Note that

$$\mathcal{W}(x) + \ln \mathcal{W}(x) = \ln x \quad \text{for } x > 0. \tag{A3}$$

By implicit differentiation, one can show that the Lambert function satisfies the differential equation

$$\frac{d\mathcal{W}}{dx} = \frac{1}{x + e^{\mathcal{W}}(x)} \quad \text{for } x \neq -1/e. \tag{A4}$$

Other useful relations are

$$\int \mathcal{W}dx = x\mathcal{W}(x) - x + e^{\mathcal{W}(x)} + c, \tag{A5}$$

and $\mathcal{W}(0) = 0$, $\mathcal{W}(e) = 1$, or

$$\int_0^e \mathcal{W}(x)dx = e - 1. \tag{A6}$$

APPENDIX B: PARTICLE PRODUCTION: ANALYTICAL ESTIMATES

In this Appendix, we estimate the range of parameters giving rise to significant particle production through the field-dependent coupling (85) in Eq. (65). For this purpose, we evaluate the adiabaticity violation parameter

$$\delta_\omega \equiv \frac{|\dot{\omega}_k|}{\omega_k^2}. \tag{B1}$$

Substantial particle production occurs if $\delta_\omega \gg 1$. For the sake of simplicity, we neglect the expansion of the Universe. In this approximation, the adiabaticity violation parameter reads

$$\delta_\omega = \frac{\sigma_h|\dot{\phi}|}{2}\frac{M_P^2(\epsilon(\phi) - \epsilon_\infty)}{(k^2 + \epsilon(\phi)M_P^2)^{3/2}}\frac{(1 - Y_\epsilon(\phi))}{\phi}. \tag{B2}$$

For $\epsilon_\infty \neq 0$ and/or $k \neq 0$, particle production is restricted to a compact field range. The maximum violation of adiabaticity for a given k happens at a field value $\phi_{\max}$ satisfying

$$\epsilon(\phi_{\max}) - \epsilon_\infty = 2\left(\epsilon_\infty + \frac{k^2}{M_P^2}\right)\Upsilon, \tag{B3}$$

with

$$\Upsilon = 1 - \frac{3}{2 + \sigma_h(1 + Y_\epsilon(\phi_{\max}))}. \tag{B4}$$

This equation cannot be generically solved for $\phi_{\max}$. In the limit $\sigma_h(1 + Y_\epsilon(\phi_{\max})) \gg 1$, we can extract an approximate field value,

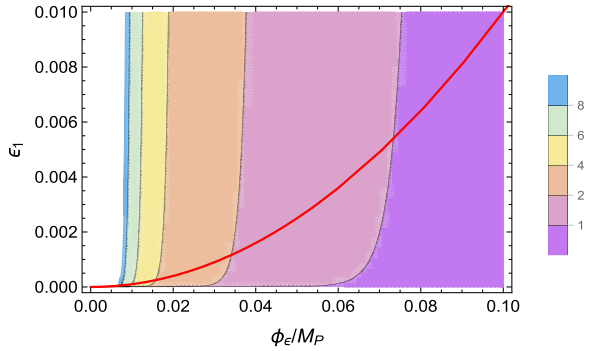

FIG. 13. Contour plot of the adiabaticity violation parameter δ_ω according to Eq. (B7) in the plane of parameters ϕ_ϵ and ϵ_1. For the other parameters, we employ $\sigma_h = 2$, $\epsilon_\infty = 10^{-10}$, a typical field velocity $|\dot{\phi}(\phi_a^{\max})| = 6 \times 10^{-6} M_P^2$, and $k = 10^{-4} M_P$. The violation of adiabaticity increases toward smaller ϕ_ϵ. The red solid line corresponds to $\epsilon_1 M_P^2 = \phi_\epsilon^2$.

$$\frac{\phi_a^{\max}}{\phi_\epsilon} \approx \frac{1 - Y_a^{\max}}{\sqrt{Y_a^{\max}}}, \tag{B5}$$

with $Y_a^{\max}$ the Lambert function

$$Y_a^{\max} \equiv \mathcal{W}\left[\left(\frac{\epsilon_1 M_P^2}{2(k^2 + \epsilon_\infty M_P^2)}\right)^{2/\sigma_h}\right]. \tag{B6}$$

At this field value, we have

$$\delta_\omega\Big|_{\phi_a^{\max}} \approx \frac{\sigma_h |\dot{\phi}(\phi_a^{\max})|}{3\sqrt{3}\phi_\epsilon} \sqrt{\frac{Y_a^{\max}}{k^2 + \epsilon_\infty M_P^2}}. \tag{B7}$$

The typical values of the adiabaticity violation parameter δ_ω for $\sigma_h = 2$, a typical field velocity $|\dot{\phi}(\phi_a^{\max})| = 6 \times 10^{-6} M_P^2$ and $k = 10^{-4} M_P$ are illustrated in Fig. 13. The red solid line corresponds to $\epsilon_1 M_P^2 = \phi_\epsilon^2$. As is clearly appreciated in this figure, a significant production of highly energetic particles requires small values of ϕ_ϵ/M_P.

APPENDIX C: COSMON PRODUCTION

As any other particle coupled to the background field ϕ, cosmon excitations can be created via violations of the adiabaticity condition in the heating stage after inflation. If significantly produced, the small mass of the cosmon makes it a potential candidate for contributing to the effective number of relativistic degrees of freedom at BBN and later.

In Fourier space, the cosmon perturbations $\delta\phi$ satisfy a mode equation,

$$\ddot{\delta\phi}_k + \left(\frac{k^2}{a^2} + M_c^2(\phi)\right)\delta\phi_k = 0, \tag{C1}$$

with $M_c^2(\phi) = M_P^4 V_{,\phi\phi}$ an effective mass term constructed out of the exact cosmon potential (15). During the inflationary stage, the main contribution to this mass term is given by Eq. (90). Due to the crossover, it changes more rapidly at the end of inflation and in the early kinetic domination period. From Eq. (C1), the energy density transferred into cosmon excitations at the onset of the kinetic regime can be computed by the techniques presented in Sec. VI B. We obtain

$$\frac{\rho_{\delta\phi}^{\rm kin}}{\rho_\phi^{\rm kin}} \simeq 7 \times 10^{-17}. \tag{C2}$$

Taking into account the results in Table II and associating them to the production of Standard Model degrees of freedom ($\rho_{\rm h}^{\rm kin} \simeq \rho_{\rm SM}^{\rm kin}$), Eq. (C2) translates into a ratio,

$$3 \times 10^{-8} \geq \frac{\rho_{\delta\phi}^{\rm kin}}{\rho_{\rm SM}^{\rm kin}} \geq 5.3 \times 10^{-11}, \tag{C3}$$

for values of ϕ_ϵ in the range $10^{-4} \leq \phi_\epsilon \leq 10^{-1}$.

Additional relativistic degrees of freedom on top of the Standard Model ones are typically parametrized in terms of an effective number of neutrinos at BBN,

$$\Delta N_{\rm eff} \equiv \frac{\rho_\phi^{\rm BBN}}{\rho_\nu^{\rm BBN}}, \tag{C4}$$

with $\rho_\nu = \frac{\pi^2}{30} g_\nu T_{\rm f}^4$ the energy density associated to a single neutrino species. Assuming complete thermalization at the onset of kinetic domination and taking into account the scaling of the different components, this quantity can be easily related to $\rho_{\delta\phi}^{\rm kin}/\rho_{\rm SM}^{\rm kin}$ up to an order 1 numerical factor associated to the change of relativistic degrees of freedom from the onset of kinetic domination to the BBN era (for details see Ref. [11]),

$$\Delta N_{\rm eff} \propto \frac{\rho_{\delta\phi}^{\rm kin}}{\rho_{\rm SM}^{\rm kin}}. \tag{C5}$$

We conclude therefore that the contribution of cosmon excitations (C3) to the effective number of neutrinos at BBN is tiny, well within the cosmological bound $\Delta N_{\rm eff} \lesssim 0.15 \pm 0.23$ provided by the Planck Collaboration [33]. The cosmon remains an elusive particle that cannot be detected by any astrophysical or particle physics experiment. Only its field value at large scales, from the horizon perhaps down to cluster scales, is accessible to observation.

[1] C. Wetterich, Nucl. Phys. **B302**, 668 (1988).
[2] B. Ratra and P. J. E. Peebles, Phys. Rev. D **37**, 3406 (1988).
[3] P. J. E. Peebles and A. Vilenkin, Phys. Rev. D **59**, 063505 (1999).
[4] B. Spokoiny, Phys. Lett. B **315**, 40 (1993).
[5] P. Brax and J. Martin, Phys. Rev. D **71**, 063530 (2005).
[6] M. Shaposhnikov and D. Zenhausern, Phys. Lett. B **671**, 162 (2009).
[7] Y. Fujii, Phys. Rev. D **9**, 874 (1974).
[8] Y. Fujii, Phys. Rev. D **26**, 2580 (1982).
[9] M. Shaposhnikov and D. Zenhausern, Phys. Lett. B **671**, 187 (2009).
[10] J. Garcia-Bellido, J. Rubio, M. Shaposhnikov, and D. Zenhausern, Phys. Rev. D **84**, 123504 (2011).
[11] J. Garcia-Bellido, J. Rubio, and M. Shaposhnikov, Phys. Lett. B **718**, 507 (2012).
[12] F. Bezrukov, G. K. Karananas, J. Rubio, and M. Shaposhnikov, Phys. Rev. D **87**, 096001 (2013).
[13] J. Rubio and M. Shaposhnikov, Phys. Rev. D **90**, 027307 (2014).
[14] G. K. Karananas and J. Rubio, Phys. Lett. B **761**, 223 (2016).
[15] P. G. Ferreira, C. T. Hill, and G. G. Ross, Phys. Lett. B **763**, 174 (2016).
[16] P. G. Ferreira, C. T. Hill, and G. G. Ross, Phys. Rev. D **95**, 043507 (2017).
[17] K. Kannike, M. Raidal, C. Spethmann, and H. Veermäe, J. High Energy Phys. 04 (2017) 026.
[18] C. Wetterich, Astron. Astrophys. **301**, 321 (1995).
[19] C. Wetterich, Nucl. Phys. **B897**, 111 (2015).
[20] C. Wetterich, Phys. Rev. D **89**, 024005 (2014).
[21] C. Wetterich, Phys. Dark Universe **2**, 184 (2013).
[22] M. W. Hossain, R. Myrzakulov, M. Sami, and E. N. Saridakis, Phys. Rev. D **90**, 023512 (2014).
[23] A. Agarwal, R. Myrzakulov, M. Sami, and N. K. Singh, Phys. Lett. B **770**, 200 (2017).
[24] S. Ahmad, R. Myrzakulov, and M. Sami, arXiv:1705.02133.
[25] C. Q. Geng, C. C. Lee, M. Sami, E. N. Saridakis, and A. A. Starobinsky, J. Cosmol. Astropart. Phys. 06 (2017) 011.
[26] C. Wetterich, Phys. Lett. B **726**, 15 (2013).
[27] J. P. Uzan, Living Rev. Relativ. **14**, 2 (2011).
[28] C. Wetterich, Phys. Lett. B **773**, 6 (2017).
[29] T. Henz, J. M. Pawlowski, and C. Wetterich, Phys. Lett. B **769**, 105 (2017).
[30] M. Abramowitz and I. A. Stegun, *Handbook of Mathematical Functions* (Dover, New York, 1965).
[31] K. Dimopoulos and C. Owen, J. Cosmol. Astropart. Phys. 06 (2017) 027.
[32] P. A. R. Ade *et al.* (Planck Collaboration), Astron. Astrophys. **594**, A20 (2016).
[33] P. A. R. Ade *et al.* (Planck Collaboration), Astron. Astrophys. **594**, A13 (2016).
[34] V. Sahni, Phys. Rev. D **42**, 453 (1990).
[35] M. Maggiore, Phys. Rep. **331**, 283 (2000).
[36] M. Giovannini, Phys. Rev. D **60**, 123511 (1999).
[37] M. Giovannini, Phys. Rev. D **58**, 083504 (1998).
[38] E. J. Chun, S. Scopel, and I. Zaballa, J. Cosmol. Astropart. Phys. 07 (2009) 022.
[39] H. Tashiro, T. Chiba, and M. Sasaki, Classical Quantum Gravity **21**, 1761 (2004).
[40] M. Sami and V. Sahni, Phys. Rev. D **70**, 083513 (2004).
[41] B. Feng and M. z. Li, Phys. Lett. B **564**, 169 (2003).
[42] K. Dimopoulos, Phys. Rev. D **68**, 123506 (2003).
[43] A. R. Liddle and L. A. Urena-Lopez, Phys. Rev. D **68**, 043517 (2003).
[44] M. Sami, N. Dadhich, and T. Shiromizu, Phys. Lett. B **568**, 118 (2003).
[45] L. H. Ford, Phys. Rev. D **35**, 2955 (1987).
[46] T. Damour and A. Vilenkin, Phys. Rev. D **53**, 2981 (1996).
[47] G. N. Felder, L. Kofman, and A. D. Linde, Phys. Rev. D **60**, 103505 (1999).
[48] C. Wetterich, Nucl. Phys. **B302**, 645 (1988).
[49] C. Wetterich, arXiv:hep-ph/0302116.
[50] J. Lachapelle and R. H. Brandenberger, J. Cosmol. Astropart. Phys. 04 (2009) 020.
[51] C. Wetterich, Phys. Rev. D **92**, 083507 (2015).
[52] L. Kofman, A. D. Linde, and A. A. Starobinsky, Phys. Rev. D **56**, 3258 (1997).
[53] P. B. Greene and L. Kofman, Phys. Lett. B **448**, 6 (1999).
[54] P. B. Greene and L. Kofman, Phys. Rev. D **62**, 123516 (2000).
[55] G. N. Felder, L. Kofman, and A. D. Linde, Phys. Rev. D **59**, 123523 (1999).
[56] R. J. Scherrer and A. A. Sen, Phys. Rev. D **77**, 083515 (2008).
[57] T. Chiba, A. De Felice, and S. Tsujikawa, Phys. Rev. D **87**, 083505 (2013).
[58] E. J. Copeland, A. R. Liddle, and D. Wands, Phys. Rev. D **57**, 4686 (1998).
[59] C. L. Reichardt, R. de Putter, O. Zahn, and Z. Hou, Astrophys. J. **749**, L9 (2012).
[60] J. L. Sievers *et al.* (Atacama Cosmology Telescope Collaboration), J. Cosmol. Astropart. Phys. 10 (2013) 060.
[61] V. Pettorino, L. Amendola, and C. Wetterich, Phys. Rev. D **87**, 083009 (2013).
[62] P. A. R. Ade *et al.* (Planck Collaboration), Astron. Astrophys. **594**, A14 (2016).
[63] M. Doran, J. M. Schwindt, and C. Wetterich, Phys. Rev. D **64**, 123520 (2001).
[64] C. Wetterich, Phys. Lett. B **655**, 201 (2007).
[65] L. Amendola, M. Baldi, and C. Wetterich, Phys. Rev. D **78**, 023015 (2008).
[66] R. Fardon, A. E. Nelson, and N. Weiner, J. Cosmol. Astropart. Phys. 10 (2004) 005.
[67] A. W. Brookfield, C. van de Bruck, D. F. Mota, and D. Tocchini-Valentini, Phys. Rev. D **73**, 083515 (2006); **76**, 049901(E) (2007).
[68] D. F. Mota, V. Pettorino, G. Robbers, and C. Wetterich, Phys. Lett. B **663**, 160 (2008).
[69] S. Casas, V. Pettorino, and C. Wetterich, Phys. Rev. D **94**, 103518 (2016).